AD-A231 340

Final Report
for the period
2 March 1987 to
31 May 1987

Theoretical Studies of Highly Energetic CBES Materials

December 1990

Authors:
N.E. Brener
N.R. Kestner
J. Callaway

Louisiana State University
Department of Physcis and Astronomy
Baton Rouge LA 70803-4001

F04611-87-C-0026

DTIC
ELECTE
JAN 23 1991
S E D

Approved for Public Release

Prepared for the: **Astronautics Laboratory (AFSC)**
Air Force Space Technology Center
Space Systems Division
Air Force Systems Command
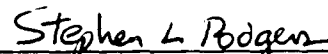Edwards AFB CA 93523-5000

NOTICE

When U.S. Government drawings, specifications, or other data are used for any purpose other than a definitely related Government procurement operation, the fact that the Government may have formulated, furnished, or in any way supplied the said drawings, specifications, or other data, is not to be regarded by implication or otherwise, or in any way licensing the holder or any other person or corporation, or conveying any rights or permission to manufacture, use or sell any patented invention that may be related thereto.

FOREWORD

This final report was submitted by Louisiana State University, Baton Rouge LA on completion of contract F04611-87-K-0026 with the Astronautics Laboratory (AFSC), Edwards AFB CA. The AL Project Manager was Captain Pete Dolan.

This report has been reviewed and is approved for release and distribution in accordance with the distribution statement on the cover and on the DD Form 1473.

PETER J. DOLAN, CAPTAIN, USAF
Project Manager

STEPHEN L. RODGERS
Chief, Applied Research In Energy
Storage Office

FOR THE DIRECTOR

ROBERT C. CORLEY
Director, Aeronautical Sciences Division

REPORT DOCUMENTATION PAGE

Form Approved
OMB No. 0704-0188

1a. REPORT SECURITY CLASSIFICATION	1b RESTRICTIVE MARKINGS
Unclassified	

2a. SECURITY CLASSIFICATION AUTHORITY	3. DISTRIBUTION / AVAILABILITY OF REPORT
	Approved for public release;
2b. DECLASSIFICATION / DOWNGRADING SCHEDULE	distribution is unlimited

4. PERFORMING ORGANIZATION REPORT NUMBER(S)	5. MONITORING ORGANIZATION REPORT NUMBER(S)
	AL-TR-90-060

6a. NAME OF PERFORMING ORGANIZATION	6b. OFFICE SYMBOL (If applicable)	7a. NAME OF MONITORING ORGANIZATION
Louisiana State University		Astronautics Laboratory (AFSC)

6c. ADDRESS (City, State, and ZIP Code)	7b. ADDRESS (City, State, and ZIP Code)
Department of Physics and Astronomy	AL/LSXP
Baton Rouge Louisiana 70803-4001	Edwards AFB CA 93523-5000

8a. NAME OF FUNDING / SPONSORING ORGANIZATION	8b. OFFICE SYMBOL (If applicable)	9 PROCUREMENT INSTRUMENT IDENTIFICATION NUMBER
		F04611-87-C-0026

8c ADDRESS (City, State, and ZIP Code)	10. SOURCE OF FUNDING NUMBERS			
	PROGRAM ELEMENT NO.	PROJECT NO.	TASK NO	WORK UNIT ACCESSION NO.
	62302F	5730	008G	343380

11. TITLE (Include Security Classification)

Theoretical Studies of Highly Energetic CBES Materials (U)

12. PERSONAL AUTHOR(S)
Nathan E. Brener, Neil R. Kestner, and Joseph Callaway

13a. TYPE OF REPORT	13b. TIME COVERED	14. DATE OF REPORT (Year, Month, Day)	15. PAGE COUNT
Final	FROM 870302 TO 870531	9012	73

16. SUPPLEMENTARY NOTATION

17.	COSATI CODES		18. SUBJECT TERMS (Continue on reverse if necessary and identify by block number)
FIELD	GROUP	SUB-GROUP	High Energy Density Materials, Propellants, Ab Initio Calcula-
07	02		tions, N_2, N_4, FN_3, HN_3, Simulated Annealing

19. ABSTRACT (Continue on reverse if necessary and identify by block number)

This is the final report of a theoretical research investigation which was undertaken to identify new propellants with revolutionary performance. A general method of locating new candidates was developed. By use of this method, several candidates were identified, including N_6 and N_4, which are predicted to have better performance (specific impulse) than liquid hydrogen and oxygen. Condensed phase properties of azides and promising propellant candidates were also determined by use of a simulated annealing program.

20 DISTRIBUTION / AVAILABILITY OF ABSTRACT	21 ABSTRACT SECURITY CLASSIFICATION
☒ UNCLASSIFIED/UNLIMITED ☐ SAME AS RPT ☐ DTIC USERS	Unclassified

22a NAME OF RESPONSIBLE INDIVIDUAL	22b TELEPHONE (Include Area Code)	22c OFFICE SYMBOL
PETE DOLAN, Capt, USAF	(805) 275-5760	LSXP

DD Form 1473, JUN 86   Previous editions are obsolete.

TABLE OF CONTENTS

Accession For

NTIS GRA&I	☒
DTIC TAB	☐
Unannounced	☐
Justification	

By

Distribution/

Availability Codes

Dist	Avail and/or Special
A-1	

\

LIST OF FIGURES

LIST OF TABLES

Summary of Major Results

1. A procedure has been developed and refined for identifying new energetic molecules that are candidates for advanced propellants.

2. The above procedure has led to the identification of two candidates for advanced propellants, trans N_6 and the N_4 tetrahedron.

   A. At the CISD 6-31G* level, trans N_6 has a specific enthalpy of 13.22 MJ/kg, an average I_{sp} of 496 sec., and an activation barrier of 0.80 eV.

   B. At the CISD 6-311G(2D) level, the N4 tetrahedron has a specific enthalpy of 17.72 MJ/kg, an average I_{sp} of 574 sec., and an activation barrier of 2.72 eV.

3. A simulated annealing cluster program has been developed to study energetic molecules in the condensed phase and the adsorption of energetic molecules on surfaces.

4. The simulated annealing program has been used to calculate values of 1.3 g/cm^3 and 1.1 kcal/(mole·A^3) for the density and energy density of solid FN_3.

5. The simulated annealing program has been used to calculate stable configurations for FN_3 and HN_3 molecules on KF surfaces.

6. A fast Fourier transform program has been developed to study light atoms in solid hydrogen.

Introduction

The goal of this project is to theoretically identify new high energy density materials that have the potential to form advanced propellants. The technical effort has focused on four major areas:

1. Identification of new energetic molecules
2. Condensed phase studies of energetic molecules
3. Adsorption of energetic molecules on surfaces
4. Light atoms in solid hydrogen

Each of these areas is described in detail below. The first section describes initial screening calculations that were done on a large number of new molecules in order to determine their energy density and stability. Two promising candidates selected from these screening calculations, trans N_6 and the N_4 tetrahedron, are investigated at higher levels of theory in the following section. The next section describes simulated annealing cluster calculations which were used to study FN_3 in the condensed phase. The following section describes simulated annealing studies of the adsorption of FN_3 and HN_3 molecules on KF surfaces. A fast Fourier transform program, which has been developed to study light atoms in solid hydrogen, is discussed in the last section.

New Energetic Molecules

A procedure has been developed and refined for identifying new energetic molecules that have the potential to form advanced propellants. The standard of comparison used in these studies is the H_2-O_2 system with a specific enthalpy (ΔH) of 12.56 MJ/kg and a specific impulse (I_{sp}) in the neighborhood of 457 sec. In the first stage of this procedure, new molecules are investigated at the SCF 6-31G* level, using Gaussian 86, in order to determine their specific enthalpy, vibrational stability, and relative position on the potential energy hypersurface. Promising candidates selected from these initial screening calculations are then further studied at the SCF 6-31G* level in order to determine their activation barrier and hence stability. If a significant barrier is found, the above calculations are repeated at the SCF level using larger basis sets and are then done at the CISD level with the MESA program.

Thus far, the initial SCF 6-31G* screening calculations have been performed on 33 new molecules, all of which are shown in Figs. A1-A31 in Appendix A and Figs. 1 and 3. Figs. A32-A34 in Appendix A give SCF 6-31G* results for three known molecules which were calculated for purposes of comparison. The calculated bond lengths and angles for FN_3 (Fig. A34) agree with experimental measurements to within 5 %. In all of the screening calculations, the molecules are in the singlet state, total energies are in Hartrees, distances are in Angstroms, the heat of formation is defined with respect to diatomic molecules of the elements, and the specific enthalpy is defined as the heat of formation divided by the molecular mass. The geometry and energy of the diatomic molecules of the elements are shown in Table 1. Table 2 summarizes the results of our screening calculations on the molecules given in Figs. A1-A31. As Table 2 shows, most of these structures were found to be vibrationally unstable, insufficiently energetic, or local, rather than global, minima on the potential energy hypersurface, and hence they were not investigated further. However, two molecules, trans N_6 and the N_4 tetrahedron, have been found to be stable and highly energetic at all of the levels of calculation mentioned above, and are therefore considered to be candidates for advanced propellants. Both of these molecules were investigated at higher levels of theory, as described below. It should also be noted that two of the stable molecules given in Appendix A, N_2O_3 and HN_3O, have significant specific enthalpies and hence warrant further investigation, particularly in view of the possibility that their specific enthalpies will increase at higher levels of calculation, as we will show for the case of trans N_6 and the N_4 tetrahedron.

Table 1. SCF 6-31G* optimized geometry and total energy of the diatomic molecules used in the heat of formation calculations. Bond lengths are in Angstroms and total energies are in Hartrees.

	BOND LENGTH	TOTAL ENERGY
H_2 singlet	0.729779	-1.1268278
B_2 quintet	1.505839	-49.1575116
N_2 singlet	1.078372	-108.9439495
O_2 triplet	1.162888	-149.5982597
F_2 singlet	1.344892	-198.6777567

Table 2   Results of SCF 6-31G* calculations. The numbering of the molecules corresponds to Figs. A1-A31.

|	Specific Enthalpy (MJ/kg)	Vibrational Stability	Lower Energy Structure on the Potential Energy Hypersurface
1. Rhombic N_2H_2	30.66	unstable	Trans N_2H_2 (Fig. A16)
2. Rhombic N_2F_2	1 .11	unstable	Trans N_2F_2 (Fig. A32)
3. Rhombic N_2O_2	9.62	stable	Linear N_2O_2 (Fig. A13)
4. Rhombic N_2B_2	.49	stable	none
5. Tetrahedral N_2H_2	29.29	unstable	Trans N_2H_2 (Fig. A16)
6. Tetrahedral N_2F_2	14.10	unstable	Trans N_2F_2 (Fig. A32)
7. Tetrahedral HN_3	26.89	unstable	Hydrogen Azide (Fig. A33)
8. Tetrahedral BN_3	13.90	stable	Boron Azide (Fig. A17)
9. Tetrahedral FN_3	12.37	unstable	Fluorine Azide (Fig. A34)
10. HNO_2	8.44	stable	none
11. BNO_2	7.39	stable	none
12. FNO_2	5.08	stable	none
13. Linear N_2O_2	7.11	stable	none
14. Linear N_2B_2	5.74	stable	/ symmetric N_2B_2 (Fig. A15)
15. Asymmetric N_2B_2	4.35	stable	none
16. Trans N_2H_2	6.64	stable	none
17. Boron Azide (BN_3)	5.35	stable	none
18. N_4H_2 Ring	27.19	unstable	Trans N_4H_2 (Fig. A23)
19. N_4F_2 Ring	18.34	unstable	Trans N_4F_2 (Fig. A24)
20. N_6 Ring	11.95	stable (6-31G*) unstable (6-311G(2DF))	Trans N_6 (Fig. 1)
21. N_4B_2 Ring	9.37	unstable	Trans N_4B_2 (Fig. A25)
22. N_4O_2 Ring	8.39	unstable	N_4O_2 Boat (Fig. A31)
23. Trans N_4H_2	14.17	unstable	none
24. Trans N_4F_2	9.66	unstable	none
25. Trans N_4B_2	8.07	unstable	none
26. Trans $N_2H_2O_2$	13.65	unstable	none
27. Trans $N_2F_2O_2$	8.31	unstable	none
28. N_2O_3	10.72	stable	none
29. HN_3O	10.15	stable	none
30. N_4H_4	8.39	stable	none
31. N_4O_2 Boat	8.05	stable	none

Further Investigation of Trans N_6 and the N_4 Tetrahedron

1. Trans N_6

As reported previously[1,2], the following results have been obtained in studies of an azide-like structure called Trans N_6:

1) At the SCF 6-31G* level, trans N_6, shown in Fig. 1, is found to be highly energetic, vibrationally stable, and the global minimum on the N_6 potential energy hypersurface. In the geometry optimizations on this molecule, all possible configurations, including nonplanar and nonsymmetric structures, were allowed, but the geometry still converged to the planar symmetric (C_{2h}) configuration given in Fig. 1. Another N_6 structure, the N_6 ring, given in Fig. A20 in Appendix A, was also found to be vibrationally stable at the SCF 6-31G* level but was significantly higher in energy than trans N_6, indicating that trans N_6 is the global minimum of the N_6 system.

2) Using the heat of formation given in Fig. 1, which is defined as the total energy of trans N_6 minus the total energy of three N_2 molecules, we computed a specific enthalpy for trans N_6 of 11.13 MJ/kg and a corresponding I_{sp} of 430 sec. A larger I_{sp} value of 480 sec. was computed by the Astronautics Laboratory for the case of a trans N_6 monopropellant. Taking the average of these values, one obtains an I_{sp} of 455 sec., which is at the level of the current state-of-the-art propellant system.

3) Two larger basis sets, 6-311G* and 6-311G(2DF), have been used to perform geometry optimization and vibrational frequency calculations on both trans N_6 and the N_6 ring at the SCF level. The results of these geometry optimizations are given in Tables 3 and 4. In the case of trans N_6, all of the vibrational frequencies remain positive at both of these higher basis set levels. However, the N_6 ring exhibits one negative frequency when the largest basis set, 6-311G(2DF), is used, indicating that the N_6 ring is vibrationally unstable. This result provides further indications that trans N_6 is the global minimum or ground state of the N_6 system.

4) The transition state of trans N_6 at the SCF 6-31G* level has been found and is given in Fig. 2. This structure is a nonplanar C_2 configuration and leads to dissociation into three N_2 molecules, as expected. The trans N_6 transition state yields an activation barrier of 0.54 eV compared with the corresponding FN_3 barrier of 0.47 eV. Thus at the SCF 6-31G* level, the trans N_6 barrier is approximately the same as the FN_3 barrier, indicating that the stability of trans N_6 is comparable to that of FN_3.

Trans N$_6$
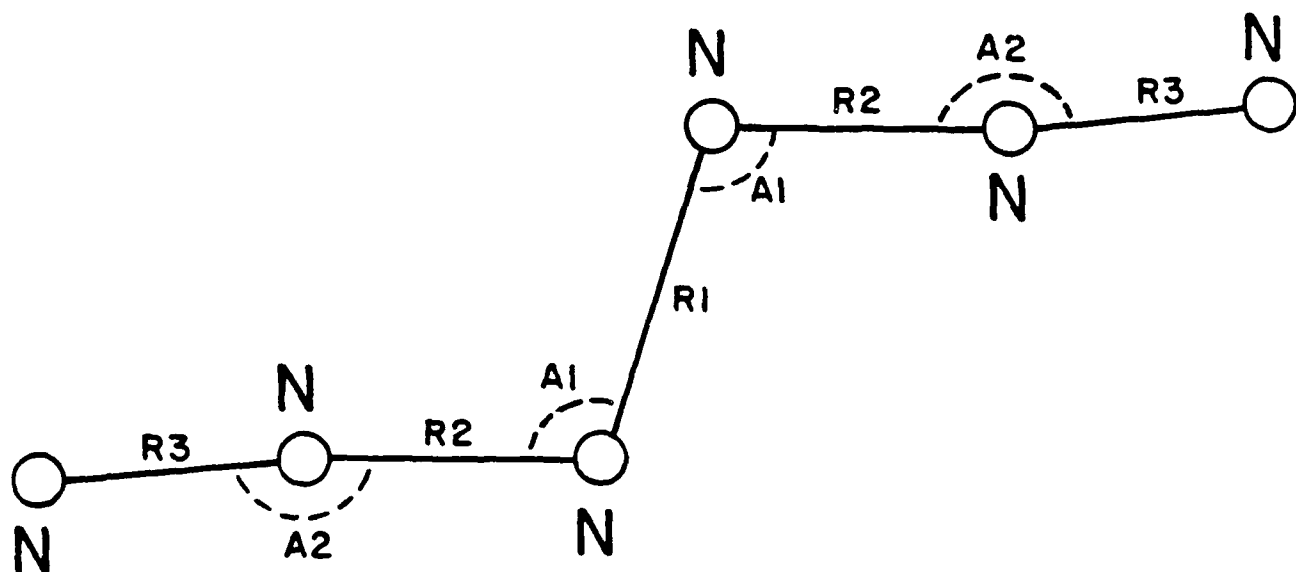
$$R1 = 1.429808$$
$$R2 = 1.235724$$
$$R3 = 1.101074$$
$$A1 = 107.378173°$$
$$A2 = 174.807741°$$
$$\text{Total Energy} = -326.4750476$$

HEAT OF FORMATION = .3568009 Hartrees = 9.7050 eV

Figure 1. SCF 6-31G* geometry and energy of trans N$_6$.

Table 3. Trans N_6 optimized geometry and total energy. The bond lengths and angles in the first columm are defined in Fig. 1.

	SCF 6-31G*	SCF 6-311G*	SCF 6-311G(2DF)
R1	1.4298	1.4285	1.4287
R2	1.2357	1.2324	1.2288
R3	1.1011	1.0945	1.0898
A1	107.38°	107.48°	107.51°
A2	174.81°	175.02°	175.19°
Total Energy	-326.47505	-326.55419	-326.58743

Table 4. N_6 ring optimized geometry and total energy. R1 is defined in Fig. A20.

	SCF 6-31G*	SCF 6-311G*	SCF 6-311G(2DF)
R1	1.2854	1.2836	1.2807
Total Energy	-326.44896	-326.52109	-326.55336

Trans N$_6$ Transition State
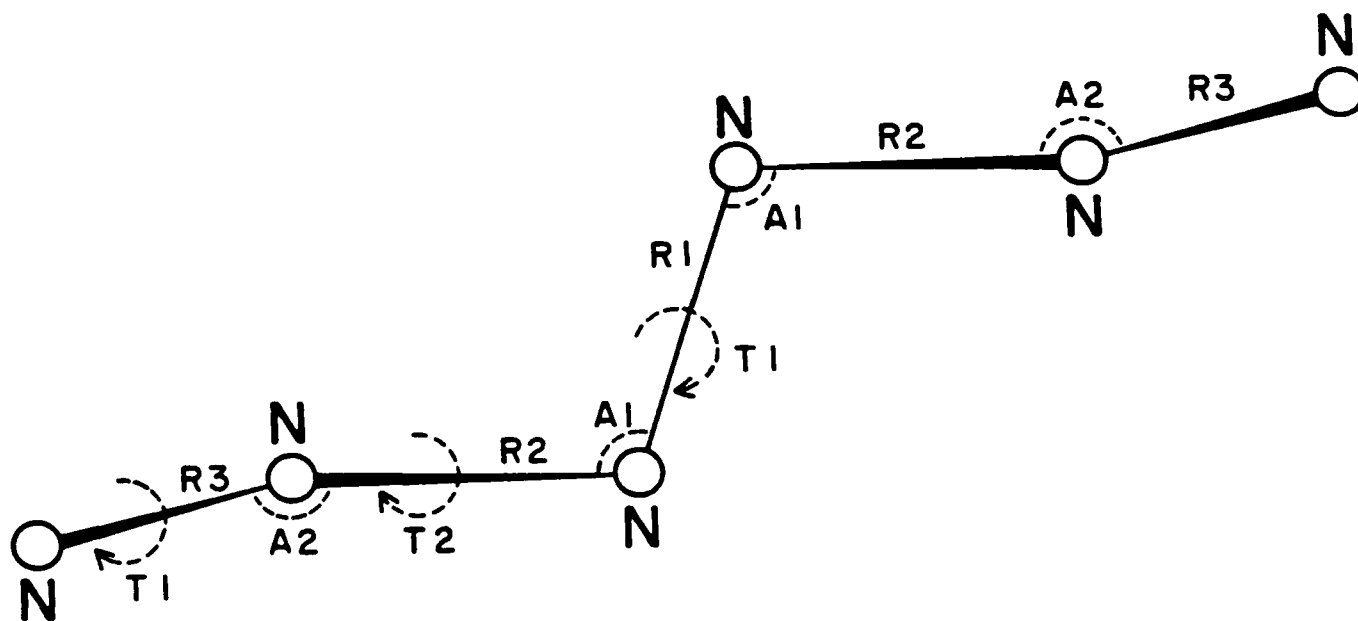
R1 = 1.35345
R2 = 1.442
R3 = 1.082699
A1 = 108.346951°
A2 = 167.059478°
T1 = 157.407856°
T2 = 98.908924°
Total Energy = -326.4553285

Figure 2. Trans N$_6$ transition state at the SCF 6-31G* level.

5) Extensive CISD calculations on trans N_6 have been carried out with the MESA program using the 6-31G* basis set and the geometries that were optimized at the SCF 6-31G* level. The results of these calculations, given in Table 5, yield a specific enthalpy for trans N_6 of 13.22 MJ/kg and a corresponding average I_{sp} of 496 sec., which is larger than the I_{sp} of the H_2-O_2 system.

6) The CISD results for trans N_6, given in Table 5, yield an activation barrier of 0.80 eV compared with the FN_3 barrier of 0.80 eV at this same level of calculation. Thus the CISD calculations again indicate that the stability of trans N_6 is approximately the same as that of FN_3 and suggest that since FN_3 has been synthesized by several research groups, the synthesis of trans N_6 should also be possible.

7) In the trans N_6 CISD calculations described above, the coefficient of the reference state, $c(0)$, is 0.91, which indicates that multi-reference CI (MRCI) calculations are not likely to produce significant changes in the above results.

8) A paper[3] has been found in which the authors report the possible synthesis of the N_6 molecule in a low temperature matrix, according to the reaction

$$cis - [Pt(N_3)_2(PPh_3)_2] \rightarrow [Pt(PPh_3)_2] + N_6$$
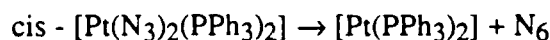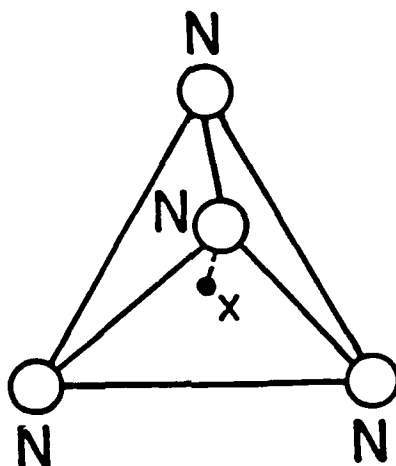
2. N_4 Tetrahedron

We have previously reported[2] the following results for the N_4 tetrahedron:

1) The N_4 tetrahedron, shown in Fig. 3 and henceforth referred to as N_4, is found to be highly energetic, vibrationally stable, and a global minimum at the SCF 6-31G* level.

2) Using the heat of formation given in Fig. 3, which is defined as the total energy of N_4 minus the total energy of two N_2 molecules, we computed a specific enthalpy for N_4 of 16.57 MJ/kg and a corresponding I_{sp} of 525 sec. By comparison with the case of trans N_6, it is estimated that an I_{sp} of 586 sec. would be obtained if N_4 is treated as a monopropellant. Taking the average of these two values, one obtains an I_{sp} of 556 sec., which is approximately 100 sec. larger than the I_{sp} of the current state-of-the-art propellant system.

13

Table 5. Trans N_6 CISD calculations.

CISD Energy

6-31G* Ground State, 447,931 Configurations   -327.24143
6-31G* Transition State, 447,931 Configurations   -327.21208

N_4 Tetrahedron

$$d_{NN} = 1.3949$$
$$\text{Total Energy} = -217.5338449$$

HEAT OF FORMATION = .3540541 Hartrees = 9.6303 eV

Figure 3. SCF 6-31G* geometry and energy of the N_4 tetrahedron. d_{NN} is the N-N distance.

3) N_4 geometry optimization and vibrational frequency calculations have also been done at the SCF 6-311G(2D) level. The resulting geometry is given in Table 6. All of the vibrational frequencies remain positive and large at this higher basis set level, with the smallest frequency increasing slightly from its 6-31G* value, indicating clearly that N_4 is stable with respect to vibration.

4) The SCF 6-311G(2D) calculations yield a specific enthalpy for N_4 of 17.26 MJ/kg and a corresponding average I_{sp} of 567 sec.

5) The N_4 transition state at the SCF level has been computed with both the 6-31G* and the 6-311G(2D) basis sets and is given in Fig. 4. This transition state leads to dissociation into two N_2 molecules, as expected. As shown in Table 7, the N_4 transition state yields 6-31G* and 6-311G(2D) activation barriers of 3.02 eV and 2.84 eV, respectively.

6) Extensive CISD calculations on N_4 have been carried out with the MESA program using both the 6-31G* and 6-311G(2D) basis sets and the geometries that were optimized at the SCF 6-31G* and SCF 6-311G(2D) levels, respectively. The resulting CISD energies, given in Table 8, yield specific enthalpies of 16.45 MJ/kg and 17.72 MJ/kg for the 6-31G* and 6-311G(2D) basis sets, respectively, and corresponding average I_{sp} values of 553 sec. and 574 sec. Thus at the highest level of calculation considered so far, the I_{sp} of N_4 is more than 100 sec. larger than the I_{sp} of the H_2-O_2 system. Table 9 summarizes the specific enthalpies and average I_{sp} values obtained for N_4 at various levels of calculation.

7) The N_4 CISD calculations yield activation barriers of 2.90 eV and 2.72 eV for the 6-31G* and 6-311G(2D) basis sets, respectively, as shown in Table 8. Thus the N_4 barrier decreases slightly at the CISD level, compared to the SCF level, but the values of the N_4 CISD barrier are still more than three times as large as the corresponding values of the FN_3 barrier, indicating that N_4 is highly stable compared to FN_3

8) In the N_4 CISD calculations described above, the coefficient of the reference state, c(0), is 0.93, which indicates that MRCI calculations are not likely to produce significant changes in the above results.

Conclusion

Both trans N_6 and the N_4 tetrahedron are stable and highly energetic at all of the levels of theory described above, and are therefore considered to be candidates for advanced propellants. We recommend that experimental research groups investigate the synthesis of both of these molecules.

Table 6. N_4 tetrahedron optimized geometry and total energy. d_{NN} is defined in Fig. 3.

	SCF 6-31G*	SCF 6-311G(2D)
d_{NN}	1.3949	1.3979
Total Energy	-217.53384	-217.58983

N$_4$ Tetrahedron Transition State
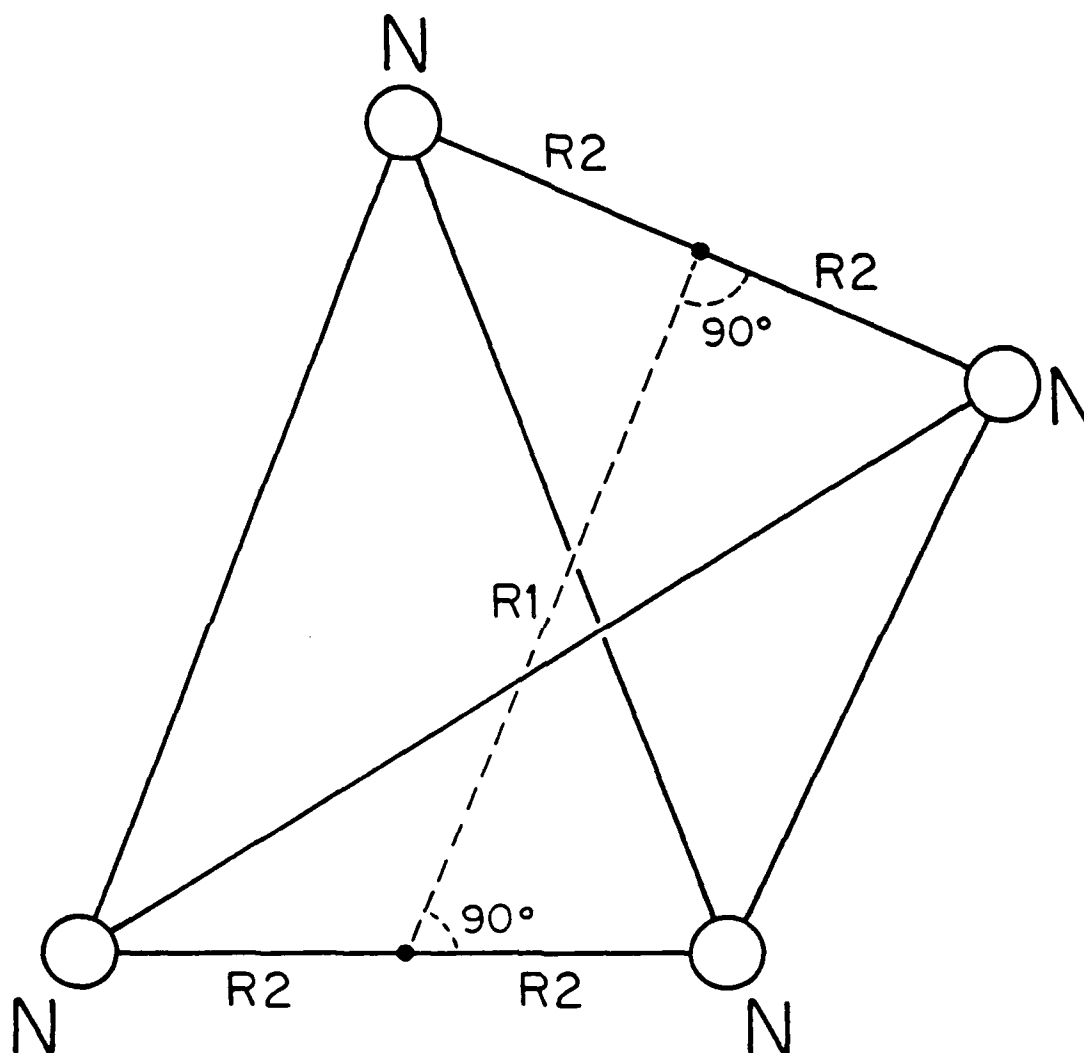
	SCF 6-31G*	SCF 6-311G(2D)
R1	1.498	1.493
R2	0.628035	0.626879
Total Energy	-217.4229495	-217.4854588

Figure 4. N$_4$ tetrahedron transition state.

Table 7. N_4 tetrahedron activation barrier.

	Barrier
SCF 6-31G*	3.02 eV
SCF 6-311G(2D)	2.84 eV
CISD 6-31G*	2.90 eV
CISD 6-311G(2D)	2.72 eV

Table 8. N_4 tetrahedron CISD calculations.

	CISD Energy
6-31G* Ground State, 88,831 Configurations	-218.09199
6-31G* Transition State, 88,831 Configurations	-217.98552
6-311G(2D) Ground State, 337,431 Configurations	-218.21259
6-311G(2D) Transition State, 337,431 Configurations	-218.11248

Table 9. N_4 tetrahedron specific enthalpy and average I_{sp}.

	Specific Enthalpy (MJ/kg)	Average I_{sp} (sec.)
SCF 6-31G*	16.57	556
SCF 6-311G(2D)	17.26	567
CISD 6-31G*	16.45	553
CISD 6-311G(2D)	17.72	574

Condensed Phase Studies of FN$_3$

A new method of geometry optimization for large clusters of molecules, the simulated annealing procedure, has recently been developed. This method, which is fast and flexible, enables one to study increasingly larger clusters of energetic molecules in order to determine the trends that occur as the cluster approaches the molecular solid. In this way one can obtain converged values for a number of condensed phase properties of interest, including the density, energy density, and binding energy per molecule. In this procedure, which simulates the process of gradually cooling the cluster from an initial high temperature, the molecular geometries are held fixed while atom-atom potentials are used to describe the interaction between each pair of atoms in the cluster. As an example of this method, results are presented for simulated annealing calculations on clusters of the FN$_3$ molecule, whose SCF 6-31G* geometry is given in Fig. A34. In these FN$_3$ studies, N-N, N-F, and F-F atom-atom potentials were determined from atomic charges computed at the CISD 6-31G* level and from N$_2$-NF and NF-NF interactions computed at the MP2 6-31G* level. The simulated Annealing program was then used to obtain optimized geometries and average molecular volumes for FN$_3$ clusters containing up to 9 molecules. As shown in Table 10, the volume per molecule was found to quickly reach a nearly constant value as the size of the cluster increases. This converged value of the molecular volume has been used to compute the density and energy density of solid FN$_3$, yielding values of 1.3 g/cm^3 and 1.1 kcal/(mole·A^3), respectively. The energy density calculation is based on the FN$_3$ heat of formation of 4.143 eV given in Fig. A34. To our knowledge, there have been no experimental measurements of the density or energy density of solid FN$_3$. As shown by Table 11, the binding energy per FN$_3$ molecule also converges rapidly with increasing cluster size, approaching an estimated converged value of 0.12 eV. Due to its speed and flexibility, the Simulated Annealing program can be applied to many energetic molecules of interest.

Table 10. Average molecular volume of clusters of FN_3 molecules.

Number of Molecules in Cluster	Volume per Molecule (A^3)
3	82.7
4	82.2
5	80.7
6	79.7
7	79.1
8	80.5
9	80.6

Density of Solid FN_3 = 1.3 g/cm^3

Energy Density of Solid FN_3 = 1.1 $kcal/(mole \cdot A^3)$

Table 11. Binding energy of clusters of FN_3 molecules.

Number of Molecules in Cluster	Binding Energy per Molecule
5	0.087 eV
6	0.097 eV
7	0.103 eV
8	0.112 eV
9	0.114 eV

Adsorption of FN_3 and HN_3 Molecules on KF Surfaces

The possible stabilization of energetic molecules by adsorption on surfaces has recently become an area of considerable interest, as this process can lead to larger I_{sp} values for solid propellants if the substrate is also an energetic substance. In this regard, Dr. Stephen Rodgers of the Astronautics Laboratory has shown that the I_{sp} yield of ammonium perchlorate (AP), which is the current state-of-the-art solid propellant, could be increased by the adsorption of FN_3 molecules on AP substrates.[4] In order to gain insight into this potentially important process, the Astronautics Laboratory has carried out experimental studies of azide molecule adsorption on alkali-halide surfaces. In these studies it was found that FN_3 and HN_3 molecules stick to several alkali-halide surfaces, including KF, but not to others such as NaF and LiF. In order to explain these experimental results and gain an understanding of the mechanism of azide molecule surface adsorption, we used the Simulated Annealing program to study the adsorption of FN_3 and HN_3 molecules on KF surfaces. In these simulated annealing calculations, the geometry of the adsorbed molecule was held fixed while atom-ion potentials were used to describe the interaction between the azide molecule and the surface ions. The $F-K^+$, $F-F^-$, $N-K^+$, $N-F^-$, $H-K^+$, and $H-F^-$ atom-ion potentials used in these studies were determined from atomic charges computed at the CISD 6-31G* level and from F_2-K^+, F_2-F^-, N_2-K^+, N_2-F^-, H_2-K^+, and H_2-F^- interactions computed at the MP2 6-31G* level. The Simulated Annealing program was then used to optimize the geometry of the system, yielding stable configurations for both FN_3 and HN_3. Two different views of each of these configurations are given in Figs. 5 and 6 (FN_3) and Figs. 7 and 8 (HN_3). As shown by the figures, the F atom in FN_3 is found to be directly above a K^+ ion while the H atom in HN_3 is found to be directly above an F^- ion, as expected. In both cases the line of the three nitrogen atoms is nearly parallel to the surface.
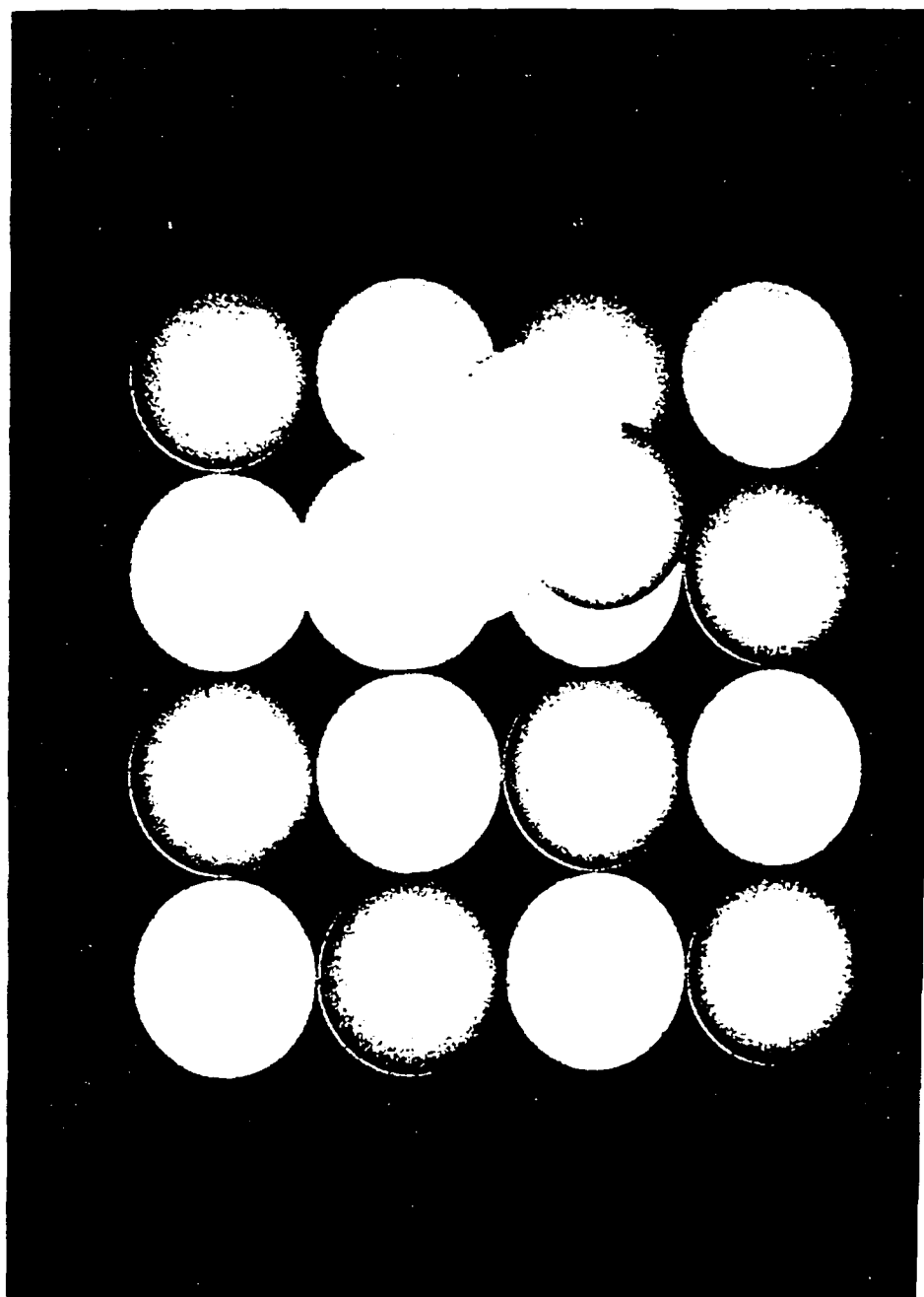
Figure 5. FN_3 molecule on KF surface. The K^+ (F^-) surface ions are pink (green).
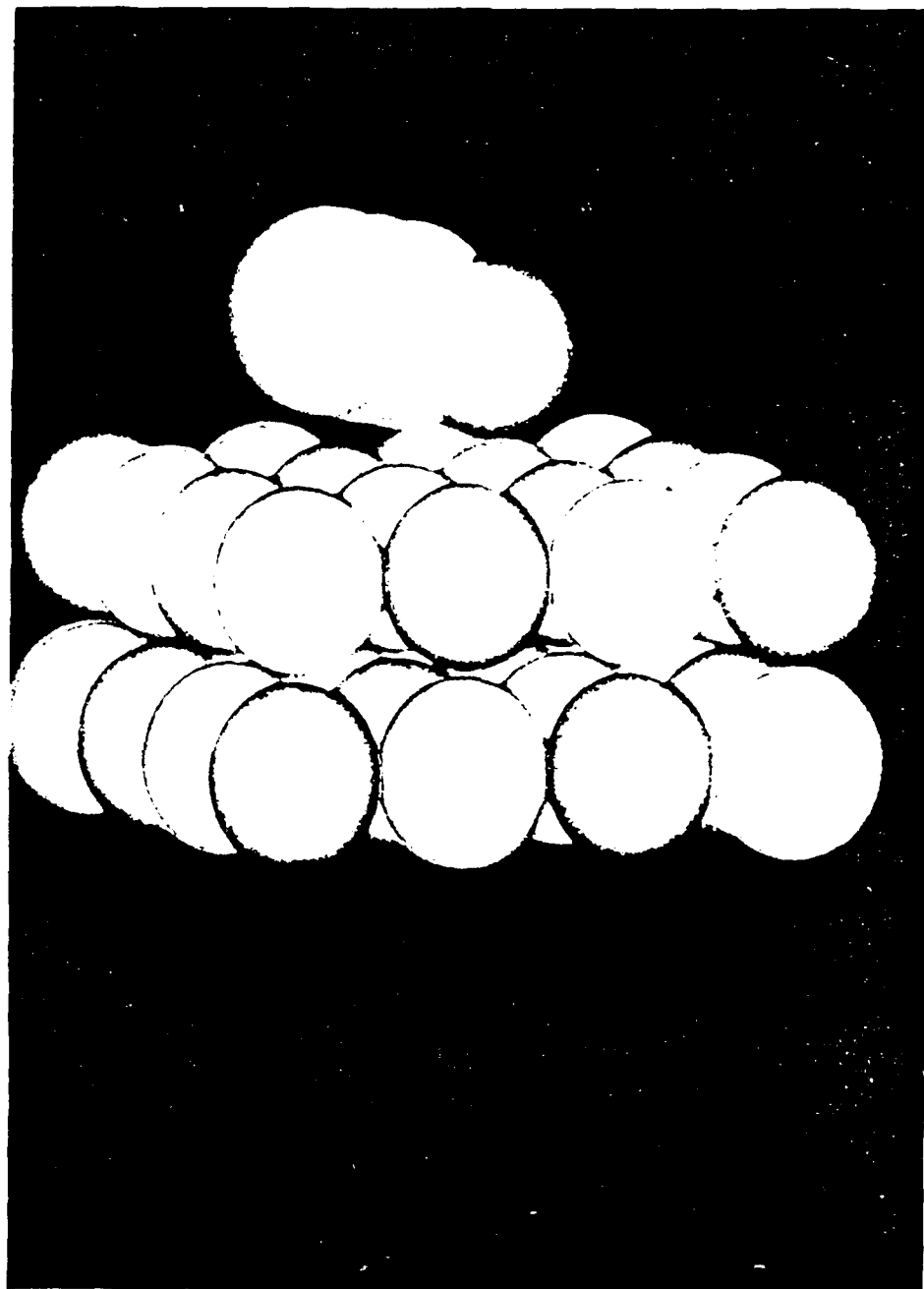
Figure 6. FN_3 molecule on KF surface. The K^+ (F^-) surface ions are pink (green).
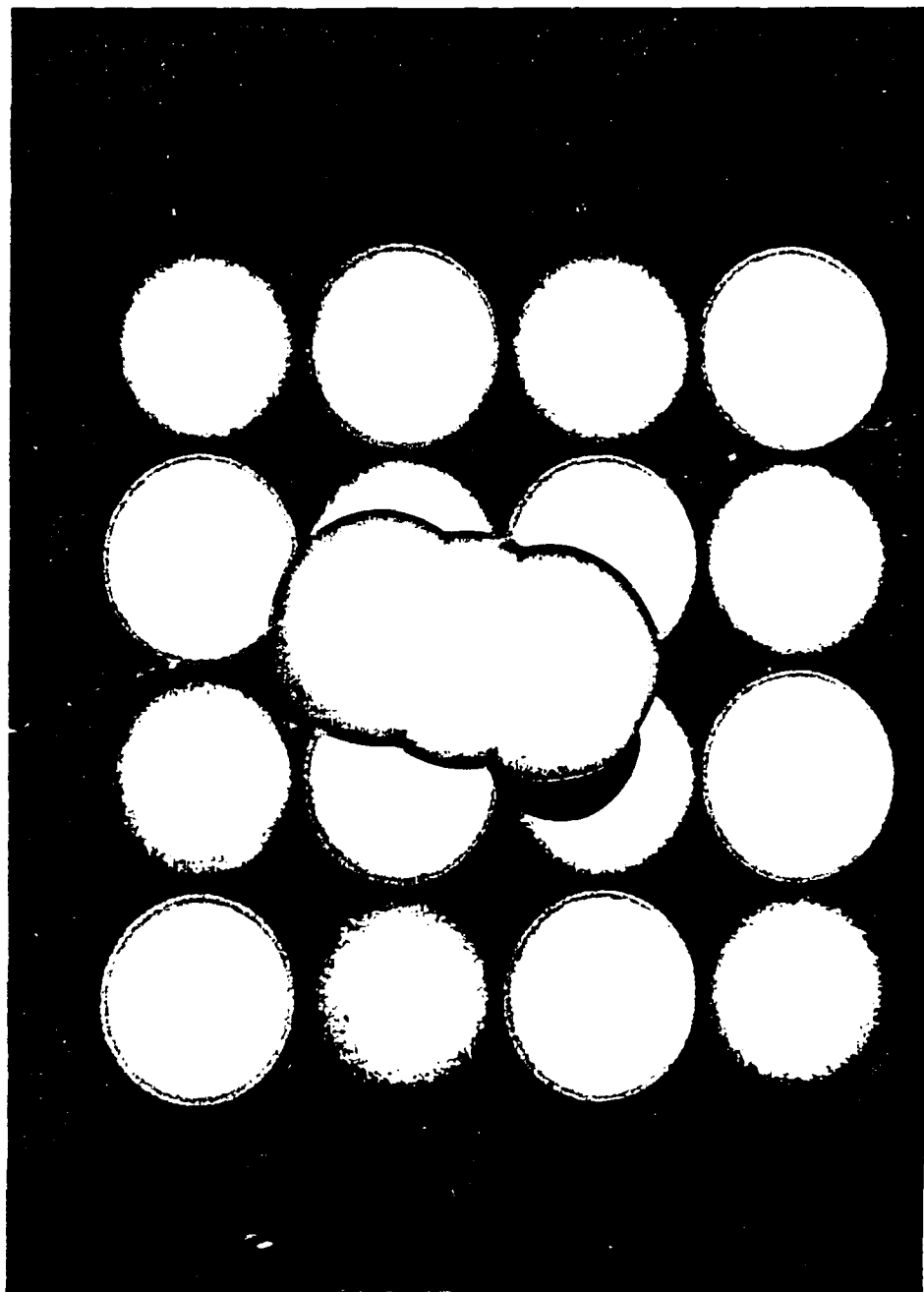
Figure 7. HN_3 molecule on KF surface. The K^+ (F^-) surface ions are pink (green).
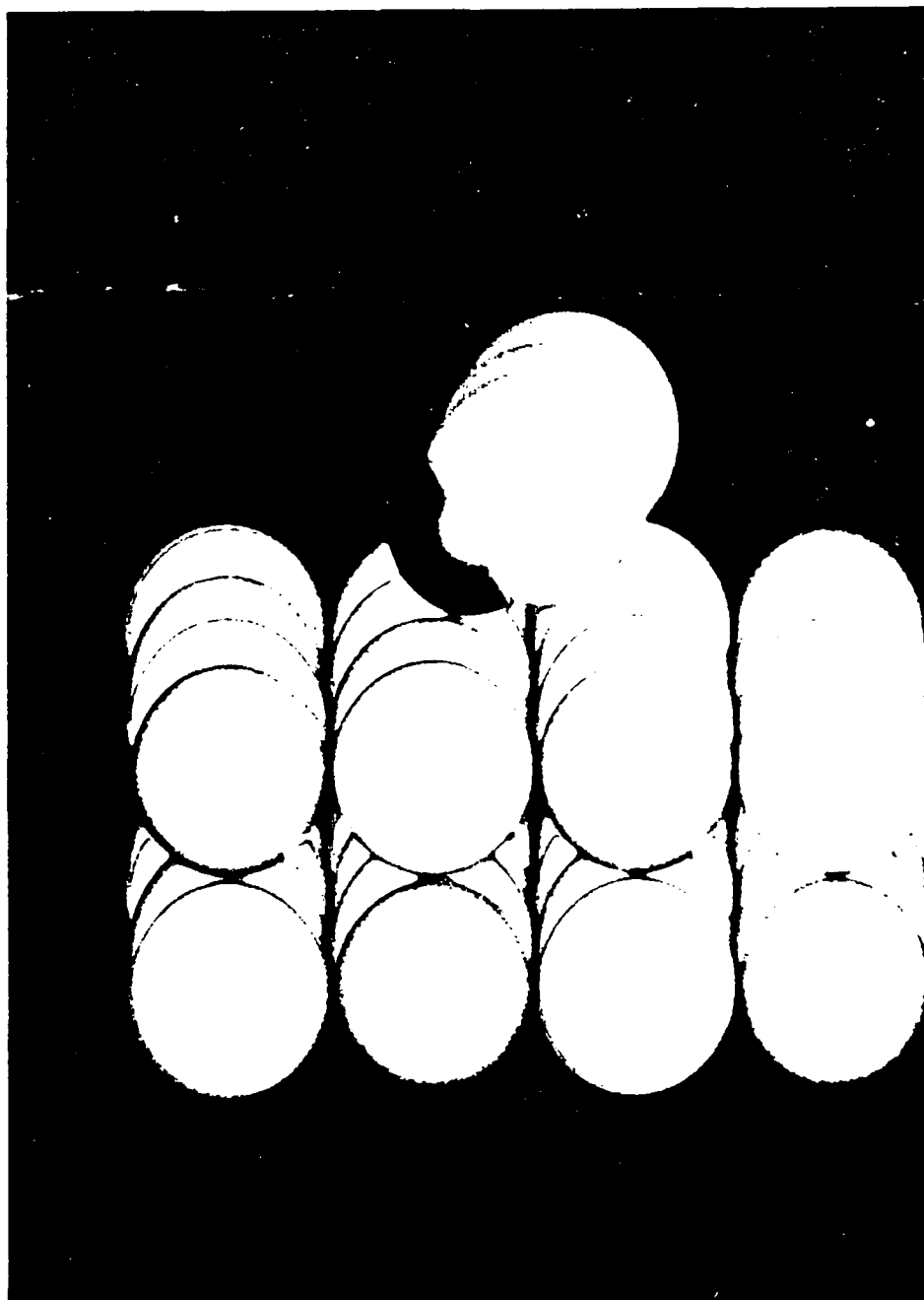
Figure 8. HN$_3$ molecule on KF surface. The K$^+$ (F$^-$) surface ions are pink (green).

Light Atoms in Solid Hydrogen

Studies have recently been performed on the trapping of light atoms, particularly Li atoms, in solid hydrogen. Such systems can yield significant I_{sp} values if the density of the trapped Li atoms is relatively large and the Li atoms can be prevented from clustering. Recent HEDM experiments involving rare gas solids have shown that this type of trapping can occur if an initial gas mixture of Li atoms and host particles is rapidly cooled. In preliminary theoretical studies of Li in solid H_2, carried out with the Simulated Annealing program, we found that the trapped Li atom is surrounded by a relatively large hole. The size of this hole would make it difficult for the Li atom to move through the H_2 solid, particularly if vacancies and defects are present as might be expected in the case of rapid cooling. Thus these initial calculations suggest that diffusion effects are not likely to be significant in this type of system and indicate that such systems have the potential to form stable energetic materials. In addition to the Simulated Annealing program, a Fast Fourier Transform program has recently been developed to study the spectra of the trapped Li atoms. A description of this program and the results of spectra calculations on Li atoms in xenon, a prototype system, are given below.

It is well known that doping lithium or other light elements into hydrogen can significantly boost its specific impulse. Work is now underway at Edwards Air Force Base, Astronautics Laboratory, to experimentally study these systems and their prototypes, namely alkali atoms in inert gases. But in order to characterize these new compositions, their properties must be understood and there must be diagnostic tools available to identify the state of the atom. We are now developing such tools and already have results for lithium in xenon and helium, media which serve as extreme test cases. During the past few years a number of new interrelated techniques have been developed to handle just this type of problem. They represent major advances in computational techniques. These new methods also take advantage of the vector and parallel architectures of the new supercomputers.

Consider the electronic absorption spectrum of a molecule or atom in some condensed phase, some disordered medium (it is just as easy to study the vibrational structure). Based on the Franck Condon Principle, we need the excitation energy for that molecule in all of the thermally accessible configurations of the medium, but, in particular, all thermally accessible configurations of the solvent around the molecule since the effect of the medium is usually relatively short range. If we could calculate this we would then have the inhomogeneously broadened line shape as the configurational average of the excitation energy for each of the possible configurations. We can find these configurations by using standard statistical mechanical methods once the correct interactions between the molecules have been determined. Since the molecules are often not spherically symmetric we will need the complete coordinates of all molecules, not just their radial distribution function around the impurity. If the medium is ordered, we could use the crystal structure as have many previous workers. Alternatively, if one wanted to only have a general picture and the medium was rather simple, one could use methods like the Mean Spherical Approximation and consider the medium as a perturbation as Chandler and co-workers have done very effectively[5]. However if we want to consider cases where

28

the wave functions are distorted by the medium and the system is rather non-isotropic, then we need to consider more elaborate methods.

Since the number of configurations we must consider is large, we need a fast way to obtain the electronic energy levels. The standard ab initio quantum chemistry techniques are much too slow to make this calculation feasible unless the number of configurations is very low and the systems very simple. The Fast Fourier Technique using the split operator method is just what is needed. Since the problem of interest can be reduced to a quasi one electron Hamiltonian, these methods are very accurate and very fast. The Fast Fourier Transform (FFT) method was originally developed by Feit, Fleck, and Kosloff[6,7]. It has been applied to many one electron or quasi one electron problems by Rossky and associates[8], by Landman and associates[9], and by Metiu and his coworkers[10], to name but a few of the major groups. There is a similarity to the approach of Carr and Parrinello[11] who evaluated systems like electrons in molten salts and most importantly, systems like liquid semiconductors. Standard quantum chemistry procedures using basis sets are also ruled out since our impurity could be altered significantly by the media as well as by temperature. We also wanted to allow for the electron density distribution to respond in any way possible, unbiased by any basis set. The FFT can also provide the lower excited states to sufficient accuracy.

The program runs were made on an IBM 3090/600S using subroutine calls to the highly vectorized ESSL (Engineering and Scientific Subroutine Library). The method scales roughly as n log n, where n is the cube of the number of points along each dimension. In order to get the energies, it is necessary to do a number of FFTs for each configuration and then propagate these in time (or imaginary time) to achieve a converged answer. This means that we need to do something of the order of 200 steps with about 2 FFTs and 2 Inverse FFTs at each time step. Nevertheless this can be done sufficiently fast so that for 16x16x16 grid points, we can get one excited state in about 12 seconds. The excited states are then found as the next orthogonal solution of the Hamiltonian, repeating the entire process. Thus we can obtain two excited states in about 20-30 seconds. This means that even for 500 or 1000 configurations three electronic states can be determined in a reasonable amount of computer time.

It might not be clear why the Fast Fourier Transform method is applicable to this problem. In principle any type of solution of those equations would be acceptable. However we will see that the FFT method is ideal. In Quantum Mechanics it is well known that one can work in either position or momentum space and solve the Schroedinger equation. The spatial representaion is preferred when dealing with coordinates or electron density distributions in space, while the momentum representation is preferred by physicists and scattering theorists who are concerned with motions of particles. It is also well known that one can transform from one represtation to another using a Fourier Transform. Also we know that the evaluation of the exponential momentum operator acting on the wave function is particulary simple if we use the momentum represention since the operator is just a number, i.e. it is diagonal in the momentum. On the other hand, the potential (V) which depends on x is most easily evaluated in the coordinate representation since V and all functions of V are then diagonal. The only

complications arise since most operators do not commute but these problems can be easily overcome by using short time steps and the split operator method.

But how do we implement this? Obviously we want to use a Fast Fourier Transform method to gain the economies of speed. We also need to discretize our space into some reasonable number of points, partly determined by the accuracy we desire. Assuming that we have the potential in some functional form or at least, evaluated at each point in our grid, let us review the steps required. One must first choose a grid size and time step which are appropriate. This generally requires some experimentation, although for a wide variety of problems which we and others have considered, a 16 point grid seems acceptable and a step size of about .3 atomic time units is also optimal. Too large a time step might lead to the wrong answer while too short a time step could cause the number of steps needed to become extremely large, and the time to be lengthened. We have found that somewhere between 100 and 200 time steps are necessary, although the program is set to stop when the necessary criterion is reached, usually about one percent in the energy.

If an excited state is desired, one chooses a new arbitrary trial function and first orthogonalizes it to the the ground state solution. In the case of finite representations of functions, such orthogonalizations are extremely fast. The results are then propagated as above. However, before being sent through another time step it is reorthogonalized to make sure it remains a pure excited state.

The program we use was originally written by U. Landman and R. Barnett at the Georgia Institute of Technology for a CDC Cyber but we modified it to use IBM ESSL routines. The speed comes from the use of the highly vectorized FFT routines, in which 256 FFTs are done at one time, and all functions are calculated only once. This is possible since we always have the same grid.

Let us now consider some of the results for lithium and sodium in inert gases. To begin we must model the Hamiltonian of an alkali in the inert gas. We have chosen to consider a simple one electron model. The alkali metal's valence electron is modeled by a simple psuedopotential composed of the Coulombic interaction with a plus one charge and an exponential repulsive term which has been fit to yield the lower excited states of the metal. In particular we use the parametrizations of Preuss[12], although we have adjusted the parameters for lithium to yield better agreement with experiment. The electron inert gas potential is also represented by a pseudopotential, which for the electron xenon and electron helium was taken from work of Berne, Coker and Thirumalai[13]. We report here only some of the early studies of sodium and lithium in xenon under various experimental conditions. Our procedure in this case is to use the previously fit inert gas-inert gas and inert gas-alkali atoms interactions (the latter by Baylis[14]) in a molecular dynamics program. We have been fortunate to have the MIXNVT program written by S. Gupta at Louisiana State University. After running the program long enough to establish equilibrium, we dump sample configurations at every tenth time step until we have collected 500 to 1000 represntative solvent configurations around the impurity. These configurations are then put into the FFT program and three or four excited states are obtained for each configuration of the molecules. The results are then expessed in terms of a histogram of the energies using either 50 or 100 bins (both are listed on the figure, the dotted lines are the 100 bin results) typically, with the range

30

covering the absorption peak. The same range is used for all densities in the results shown in Fig. 43. In order to understand these results it is important that one realize that we have used a Lennard Jones 6-12 potential for the atomic interactions and thus all results are expressed relative to those parameters. In particular the relative temperature, T_r, is expressed in terms of the well depth for the inert gas reactions. Typically a liquid or solid has T_r near one. The densities, D_r, are expressed relative to the zero of the potential cubed, or sigma cubed as it is usually expressed. It is a number density with low numbers being low densities. Only at low temperatures is the liquid state reached for relative densities, D_r, below about 0.7. The figures included in this paper represent only a brief sample of the capabilities of this method.

This method has the unique capability of going back to find out what type of configurations contribute to what features. In early work we were able to see that one case involving three distinct peaks corresponded to three distinct sets of nearest neighbor distances. Thus this method can be used to really understand some specific spectral features in molecular terms. There is currently a lot of controversy concerning the origin of the three peaks in the absorption spectra of alkali atoms in solid rare gases[15] and this method can determine whether those differences are due to different sites or splitting of excited state energies.

The extension of this method to study lithium or other alkali metals in hydrogen is straightforward. It can study in detail, effects of temperature, density, and various degrees of disorder on electronic energies. It can study a range of densities and temperatures. It can also be applied to solid state systems where the configurations will be obtained from molecular dynamics or simulated annealing results. All that is required is to implement the new potentials which are available from Dr. Konowalow at Edwards Air Force Base and also evaluate the electron hydrogen pseudopotential.

Low Density

Lithium in Xenon (Tr =2.8, Dr =.1)
2s – 2p Transition
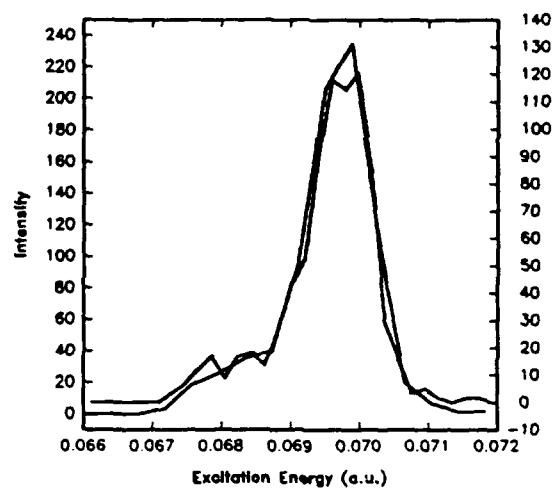
The dotted line is the more jagged one (100 bins vs 50).

Higher Density

Lithium in Xenon (Tr =2.0, Dr=.7)

2s – 2p Transition
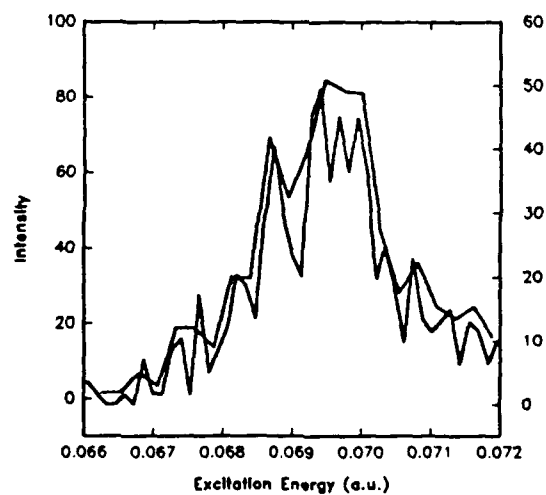
Figure 9. Lithium atoms in xenon.

References

1. N. E. Brener, J. Callaway, N. R. Kestner, and H. Chen, Proceedings of the High Energy Density Materials Conference, New Orleans, LA, March 12-15, 1989, edited by T. G. Wiley and R. A. Opijnen (Astronautics Laboratory, Edwards AFB, CA, 1989), pg. 211.

2. N. E. Brener, N. R. Kestner, J. Callaway, and H. Chen, Proceedings of the High Energy Density Materials Conference, Long Beach, CA, February 25-28, 1990.

3. A. Vogler, R. E. Wright, and H. Kunkely, Angew. Chem. Int. Ed. Engl. 19, 717 (1980).

4. S. L. Rodgers, S. D. Thompson, and R. A. Opijnen, Proceedings of the High Energy Density Materials Conference, Long Beach, CA, February 25-28, 1990.

5. K. S. Schweizer, D. Chandler, "Quantum Theory of Solvent Effects on Electronic Spectra: Prediction of the Exact Solution of the Mean Spherical Model", J. Chem. Phys. 78, 4118, (1983).

6. M. D. Feit, J. A. Fleck, Jr., "Wave Packet Dynamics and Chaos in the Henon-Heiles System", J. Chem. Phys. 80, 2578 (1984). M. D. Feit, J. A. Fleck, A. Steiger, "Solution of the Schroedinger Equation by a Spectral Method", J. Comput. Phys. 47, 412 (1982).

7. D. Kosloff, R. Kosloff, "A Fourier Method Solution for the Time Dependent Schroedinger Equation as a Tool in Molecular Dynamics", J. Comput. Phys. 52, 35 (1983).

8. J. Schnitker, K. Motakabbir, P. J. Rossky, R. Friesner, "A Priori Calculation of Optical-Absorption Spectrum of Hydrated Electron", Phys. Rev. Letters, 60, 456 (1988). J. Schnitker, P. J. Rossky, "Quantum Simulation Study of Hydrated Electron", J. Chem. Phys. 86, 3471 (1987).

9. R. N. Barnett, U. Landman, C. L. Cleveland, J. Jortner, Phys. Rev. Letters, 59, 811 (1987). R. N. Barnett, U. Landman, C. L. Cleveland, J. Jortner, "Electron Localization in Water Clusters, II. Surface and Internal States", J. Chem. Phys. 88, 4429 (1988).

10. B. Hellsing, A. Nitzan, H. Metiu, "A Fast Fourier Transform Method for Calculating the Equilibrium Density Matrix", Chem. Phys. Letters, 123, 523 (1986).

11. R. Car, M. Parrinello, "Unified Approach for Molecular Dynamics and Density-Functional Theory", Phys. Rev. Letters, 55, 478 (1985). E. Fois, A. Selloni, M. Parrinello, "Approach to Metallic Behavior in Metal-Molten-Salt Solution", Phys. Rev. B39, 4812 (1989). I. Stich, R. Car, M. Parrinello, S. Baroni, "Conjugate Gradient Minimization of the Energy Functional: A New Method for Electronic Structure Calculation", Phys. Rev. B39, 4997 (1989).

12. H. Preuss, H. Stoll, U Wedig, T. H. Kruger, "Combination of Pseudopotentials and Density Function", International. J. Quant. Chem. 19, 113 (1981).

13. D. F. Coker, B. J. Berne, D. Thirumalai, "Path Integral Monte Carlo Studies of the Behavior of Excess Electrons in Simple Fluids", J. Chem. Phys. 86, 5689 (1987).

14. W. E. Baylis, "Semiempirical, Pseudopotential Calculation of Alkali-Noble Gas Interatomic Potentials", J. Chem. Phys. 51, 2665 (1969). R. O. Watts, I. J. McGee, "Liquid State Chemical Physics", John Wiley & Son, 1976.

15. P. A. Lund, D. Smith, S. M. Jacobs, P. N. Schatz, "Magnetic Circular Dichroism Study of the $^2S \rightarrow {}^2P$ Transition of Lithium Atoms in Noble Gas Matrices", J. Phys. Chem., 88, 31 (1984). R. K. Bhargave, D. L. Dexter, "Optical Properties of Substitutional H- and Li-atom impurities in Solid Argon and Neon", Phys. Rev. B1, 1 (1970).

Appendix A

Geometry and Energy of HEDM Candidates Examined

Note: In the following figures, the molecules are in the singlet state, total energies are in
Hartrees, distances are in Angstroms, the heat of formation is defined with respect to
diatomic molecules of the elements, and the specific enthalpy is defined as the heat of
formation divided by the molecular mass.

Rhombic N_2H_2
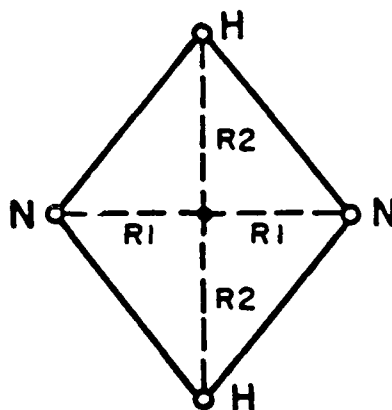
$$R1 = 0.701237$$
$$R2 = 0.905973$$
$$\text{Total Energy} = -109.7198483$$

HEAT OF FORMATION = .3509290 Hartrees = 9.5453 eV

SPECIFIC ENTHALPY = 30.66 MJ/kg

Figure A1. SCF 6-31G* geometry and energy of rhombic N_2H_2.

Rhombic N_2F_2
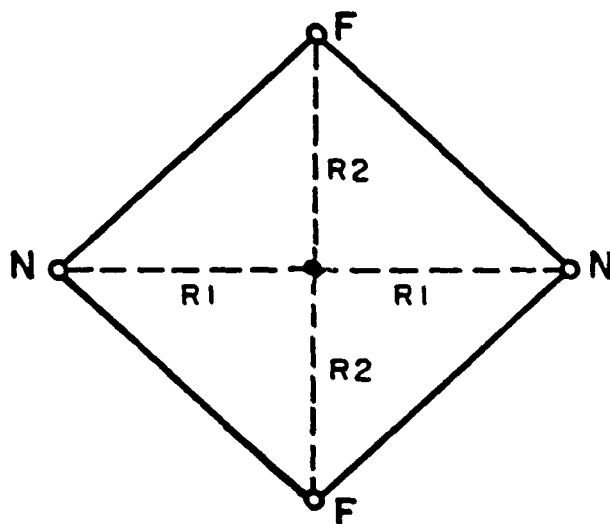
R1 $\approx$ 1.148706
R2 $\approx$ 1.061801
Total Energy $\approx$ -307.2665175

HEAT OF FORMATION $\approx$ .3551887 Hartrees = 9.6611 eV

SPECIFIC ENTHALPY $\approx$ 14.11 MJ/kg

Figure A2. SCF 6-31G* geometry and energy of rhombic N_2F_2.

Rhombic N_2O_2
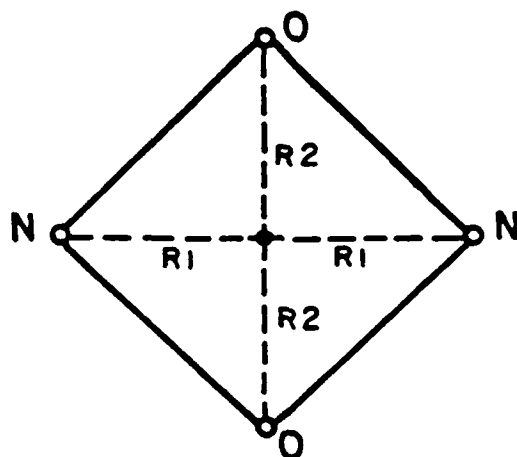
R1 = 0.938047
R2 = 0.902935
Total Energy = -258.3218875

HEAT OF FORMATION = .2203217 Hartrees = **5.9928 eV**

SPECIFIC ENTHALPY = 9.62 MJ/kg

Figure A3. SCF 6-31G* geometry and energy of rhombic N_2O_2.

Rhombic N_2B_2
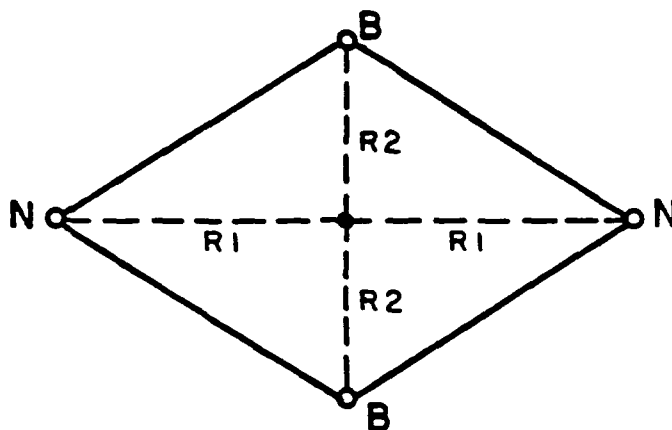
R1 = 1.167842
R2 = 0.745876
Total Energy = -158.0921921

HEAT OF FORMATION = .0092690 Hartrees = .2521 eV

SPECIFIC ENTHALPY = .49 MJ/kg

Figure A4. SCF 6-31G* geometry and energy of rhombic N_2B_2.

Tetrahedral N_2H_2
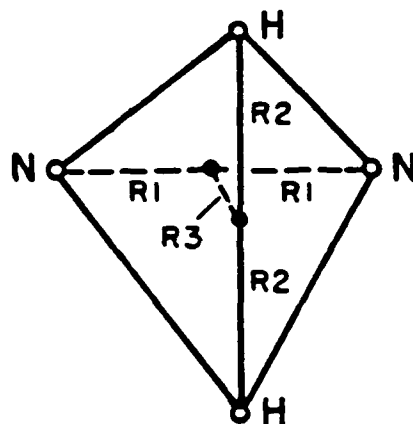
R1 = 0.681382
R2 = 0.860303
R3 = 0.454431
Total Energy = -109.7355652

HEAT OF FORMATION = .3352121 Hartrees = 9.1178 eV

SPECIFIC ENTHALPY = 29.29 MJ/kg

Figure A5. SCF 6-31G* geometry and energy of tetrahedral N_2H_2.

Tetrahedral N_2F_2
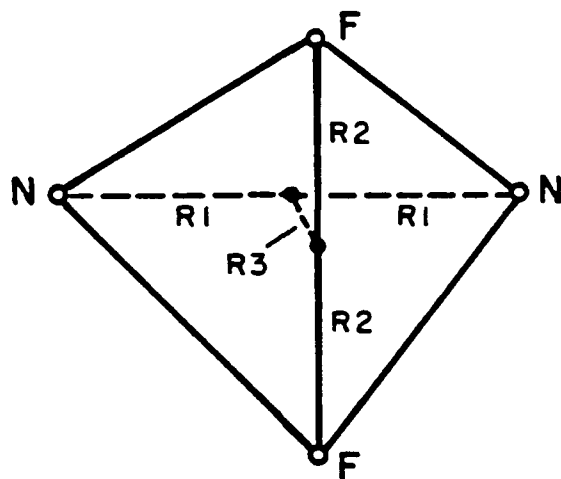
$R1 = 1.139556$
$R2 = 1.056573$
$R2 = 0.174398$
Total Energy $= -307.2666412$

HEAT OF FORMATION = .3550650 Hartrees = 9.6578 eV

SPECIFIC ENTHALPY = 14.10 MJ/kg

Figure A6. SCF 6-31G* geometry and energy of tetrahedral N_2F_2.

41
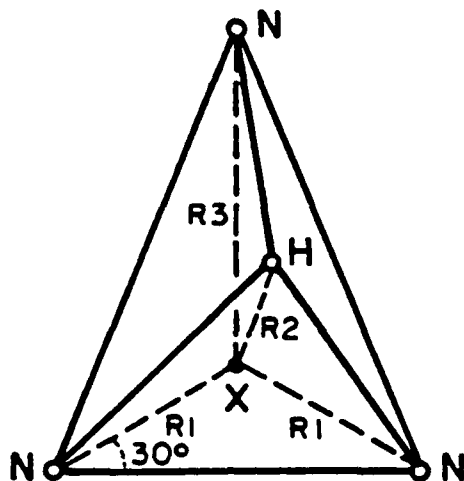
Tetrahedral HN$_3$

$$R1 = 0.701595$$
$$R2 = 1.068082$$
$$R3 = 1.105794$$
$$\text{Total Energy} = -163.5381599$$

HEAT OF FORMATION = .4411783 Hartrees = 12.0000 eV

SPECIFIC ENTHALPY = 26.89 MJ/kg

Figure A7. SCF 6-31G* geometry and energy of tetrahedral HN$_3$.

Note: In Figs. A7-A9, the point X is in the plane of the three
nitrogen atoms, and the H-X, B-X, and F-X lines are
perpendicular to this plane.

Tetrahedral BN₃
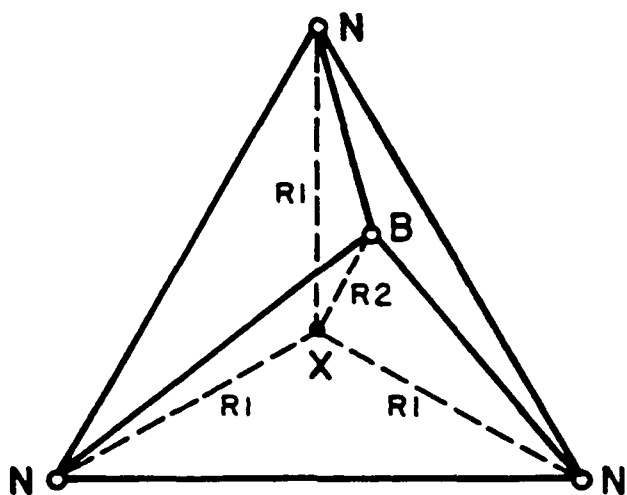
R1 = 0.882693
R2 = 1.060935
Total Energy = -187.7146720

HEAT OF FORMATION = .2800081 Hartrees = **7.6162 eV**

SPECIFIC ENTHALPY = 13.90 MJ/kg

Figure A8. SCF 6-31G* geometry and energy of tetrahedral BN₃.

Tetrahedral FN₃
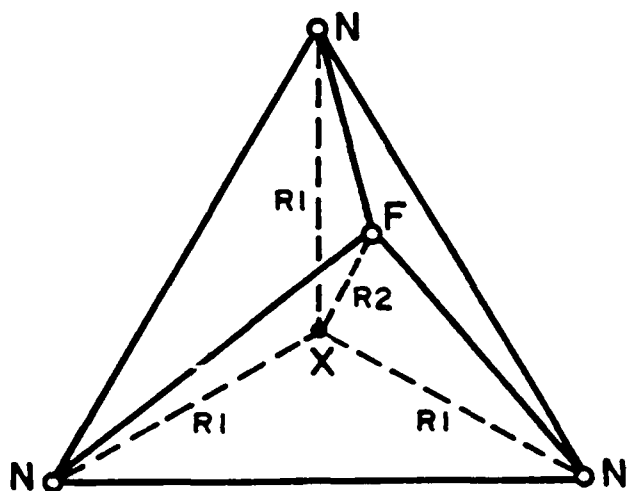
R1 = 0.7354
R2 = 1.9158
Total Energy = -262.4668922

HEAT OF FORMATION = .2879104 Hartrees = 7.8312 eV

SPECIFIC ENTHALPY = 12.37 MJ/kg

Figure A9. SCF 6-31G* geometry and energy of tetrahedral FN₃.
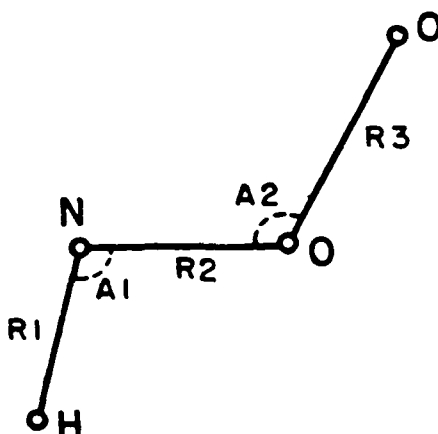
HNO$_2$

R1 = 1.013525
R2 = 1.197729
R3 = 1.301152
A1 = 104.305787°
A2 = 118.303346°
Total Energy = -204.4822336

HEAT OF FORMATION = .1514148 Hartrees = 4.1185 eV

SPECIFIC ENTHALPY = 8.44 MJ/kg

Figure A10. SCF 6-31G* geometry and energy of HNO$_2$.
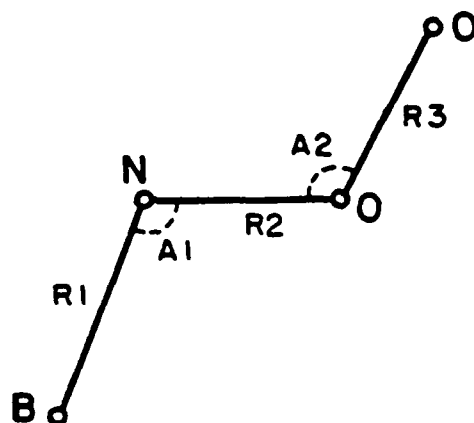
BNO$_2$

R1 = 1.466356
R2 = 1.228616
R3 = 1.235892
A1 = 111.662849°
A2 = 119.23601°
Total Energy = -228.4887084

HEAT OF FORMATION = .1602819 Hartrees = 4.3597 eV

SPECIFIC ENTHALPY = 7.39 MJ/kg

Figure A11. SCF 6-31G* geometry and energy of BNO$_2$.
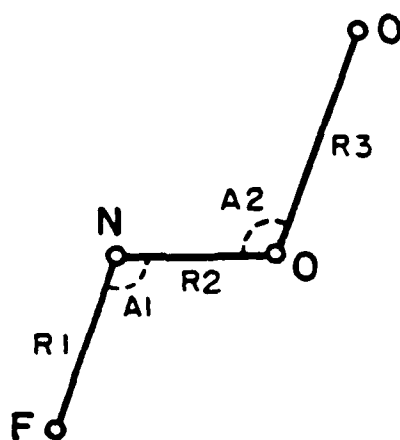
FNO$_2$

R1 = 1.338146
R2 = 1.144817
R3 = 1.703125
A1 = 109.30518°
A2 = 111.63729°
Total Energy = -303.2830799

HEAT OF FORMATION = .1260329 Hartrees = 3.4281 eV

SPECIFIC ENTHALPY = 5.08 MJ/kg

Figure A12. SCF 6-31G* geometry and energy of FNO$_2$.

Linear N_2O_2
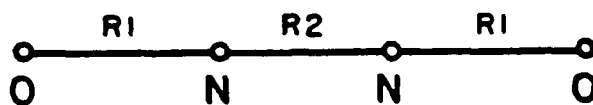
$$R1 = 1.215443$$
$$R2 = 1.081264$$
$$\text{Total Energy} = -258.3793481$$

HEAT OF FORMATION = .1628611 Hartrees = 4.4298 eV

SPECIFIC ENTHALPY = 7.11 MJ/kg

Figure A13. SCF 6-31G* geometry and energy of linear N_2O_2.

48
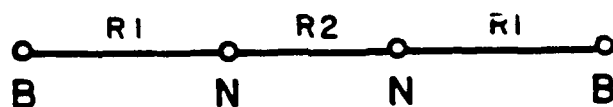
Linear N_2B_2

$$R1 = 1.406811$$
$$R2 = 1.176888$$
$$\text{Total Energy} = -157.9927275$$

HEAT OF FORMATION $= .1087336$ Hartrees $= 2.9576$ eV

SPECIFIC ENTHALPY $= 5.74$ MJ/kg

Figure A14. SCF 6-31G* geometry and energy of linear N_2B_2.

Asymmetric N_2B_2

$$R1 = 1.141336$$
$$R2 = 1.324709$$
$$R3 = 1.71895$$
$$\text{Total Energy} = -158.0191996$$

HEAT OF FORMATION = .0822615 Hartrees = 2.2375 eV

SPECIFIC ENTHALPY = 4.35 MJ/kg

Figure A15. SCF 6-31G* geometry and energy of asymmetric N_2B_2.

Trans N_2H_2
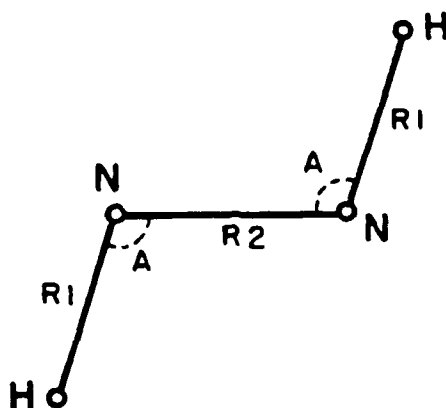
$$R1 \approx 1.014529$$
$$R2 \approx 1.215645$$
$$A \approx 107.585995°$$

Total Energy $\approx$ -109.9947653

HEAT OF FORMATION $\approx$ .0760120 Hartrees = **2.0675 eV**

SPECIFIC ENTHALPY $\approx$ **6.64 MJ/kg**

Figure A16. SCF 6-31G* geometry and energy of trans N_2H_2.

Boron Azide (BN₃)
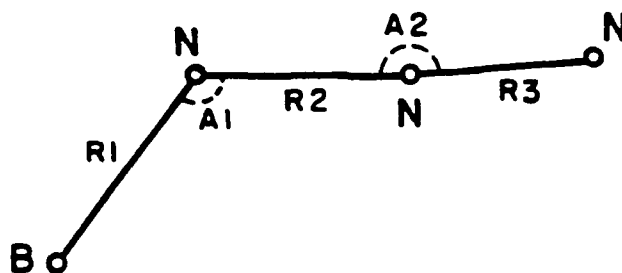
$$R1 = 1.396075$$
$$R2 = 1.231734$$
$$R3 = 1.091593$$
$$A1 = 126.873161°$$
$$A2 = 175.959388°$$
$$\text{Total Energy} = -187.8868880$$

HEAT OF FORMATION = .1077921 Hartrees = 2.9319 eV

SPECIFIC ENTHALPY = 5.35 MJ/kg

Figure A17. SCF 6-31G* geometry and energy of boron azide (BN₃).

N₄H₂ Ring
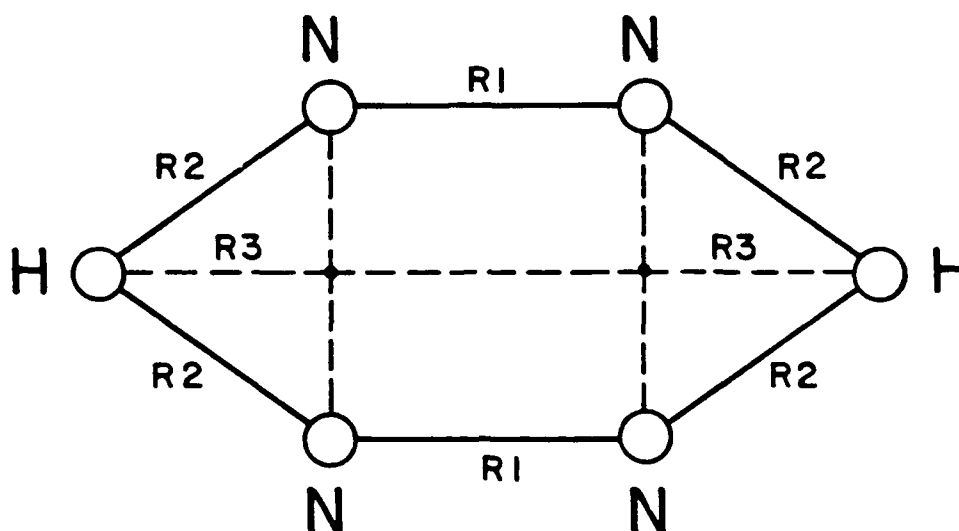
R1 = 1.298588
R2 = 1.194035
R3 = 0.972595
Total Energy = -218.4130777

HEAT OF FORMATION = .6016491 Hartrees = 16.3649 eV

SPECIFIC ENTHALPY = 27.19 MJ/kg

Figure A18. SCF 6-31G* geometry and energy of the N₄H₂ ring.

N_4F_2 Ring
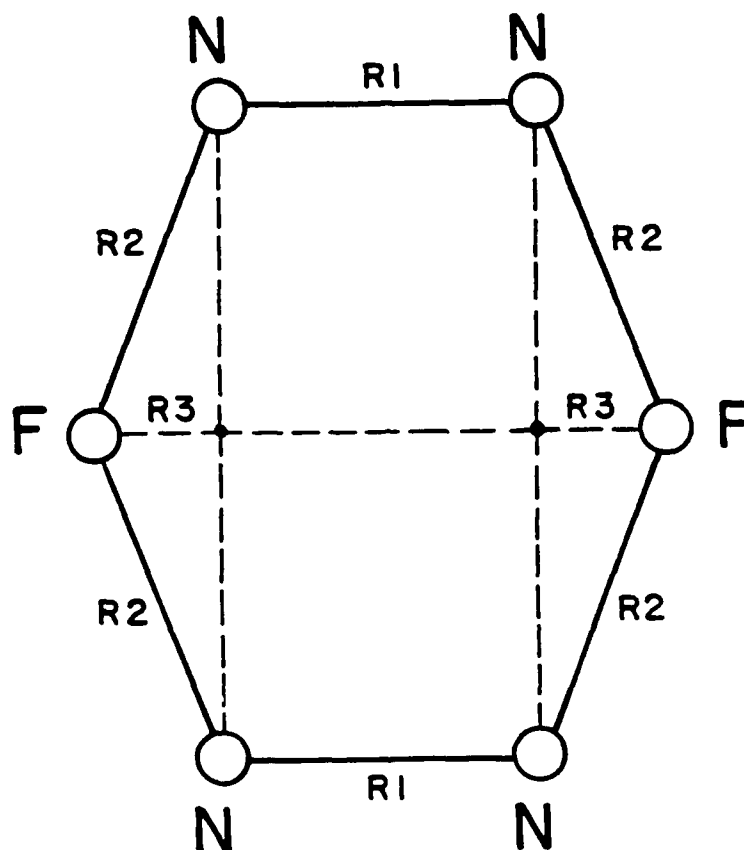
R1 = 1.317416
R2 = 1.4667
R3 = 0.537757
Total Energy = -415.9077499

HEAT OF FORMATION = .6579058 Hartrees = 17.8950 eV

SPECIFIC ENTHALPY = 18.34 MJ/kg

Figure A19. SCF 6-31G* geometry and energy of the N_4F_2 ring.

N$_6$ Ring
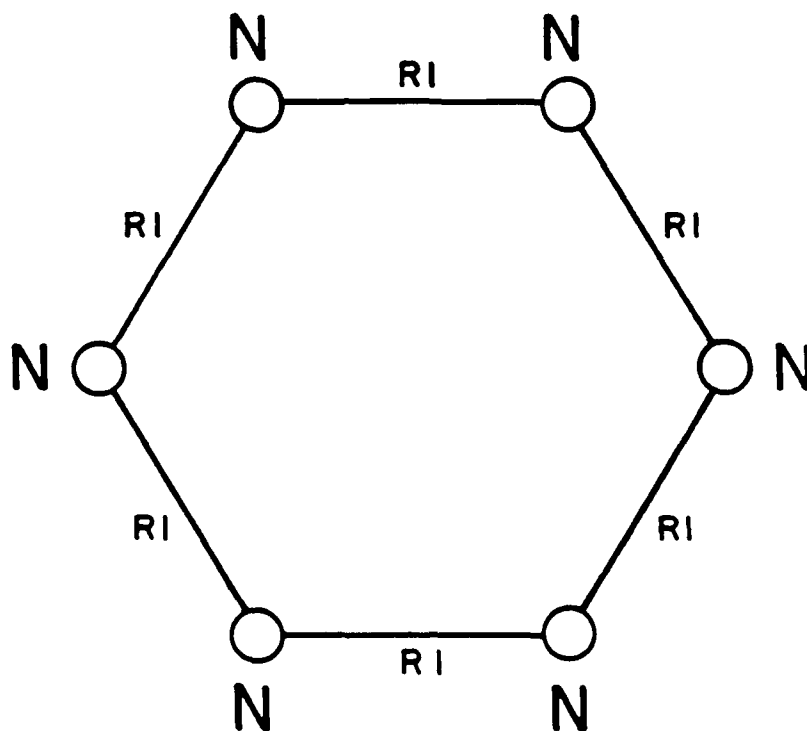
R1 = 1.285389
Total Energy = -326.4489642

HEAT OF FORMATION = .3828843 Hartrees = **10.4145 eV**

SPECIFIC ENTHALPY = 11.95 MJ/kg

Figure A20. SCF 6-31G* geometry and energy of the N$_6$ ring.

N_4B_2 Ring
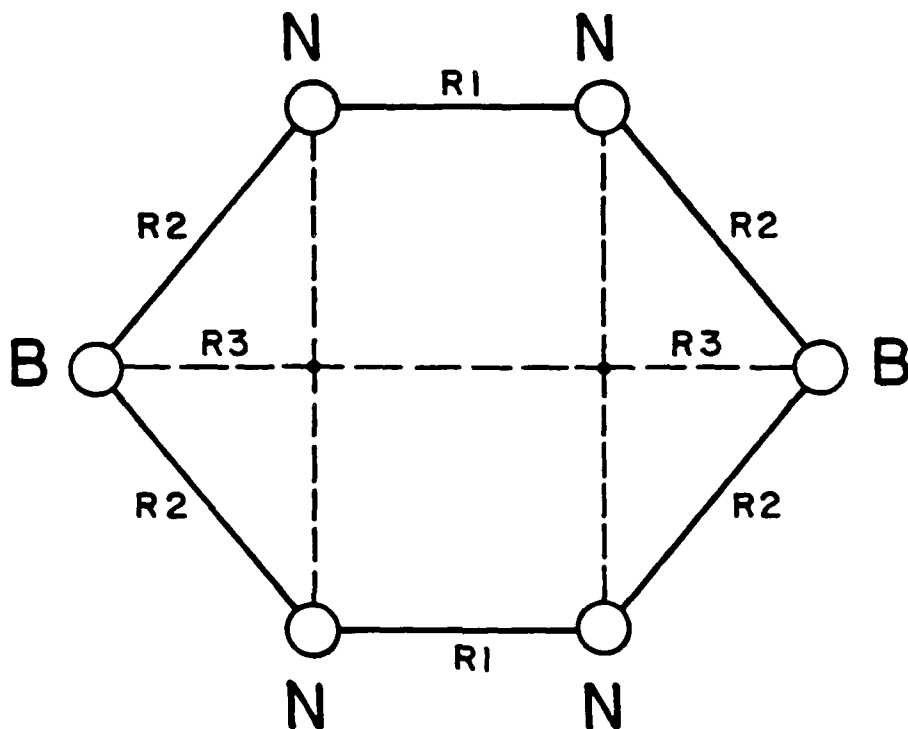
R1 = 1.19747
R2 = 1.413495
R3 = 0.902062
Total Energy = -266.7678932

HEAT OF FORMATION = .2775174 Hartrees = 7.5485 eV

SPECIFIC ENTHALPY = 9.37 MJ/kg

Figure A21. SCF 6-31G* geometry and energy of the N_4B_2 ring.

N_4O_2 Ring
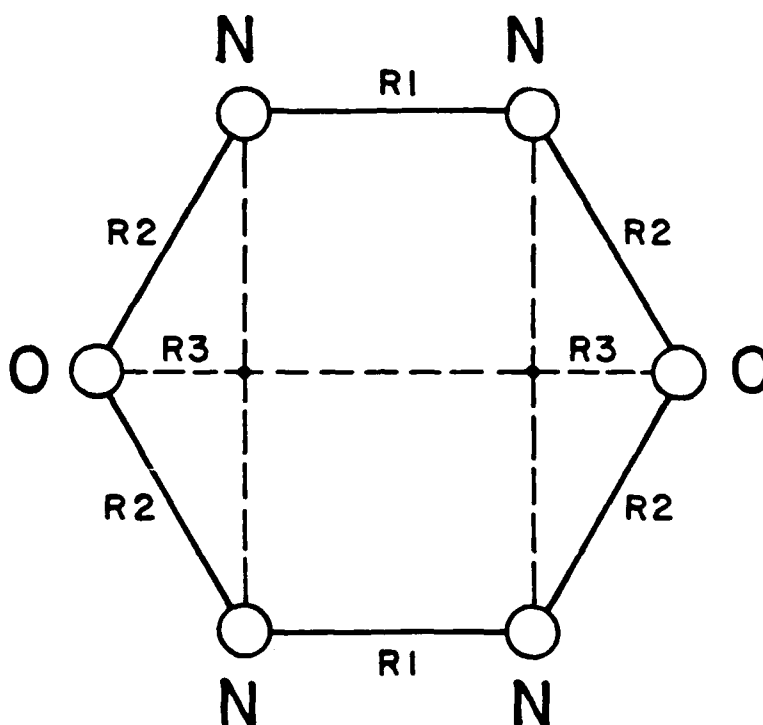
R1 = 1.195038
R2 = 1.367266
R3 = 0.679581
Total Energy = -367.2045477

HEAT OF FORMATION = .2816110 Hartrees = 7.6598 eV

SPECIFIC ENTHALPY = 8.39 MJ/kg

Figure A22. SCF 6-31G* geometry and energy of the N_4O_2 ring.

Trans N_4H_2
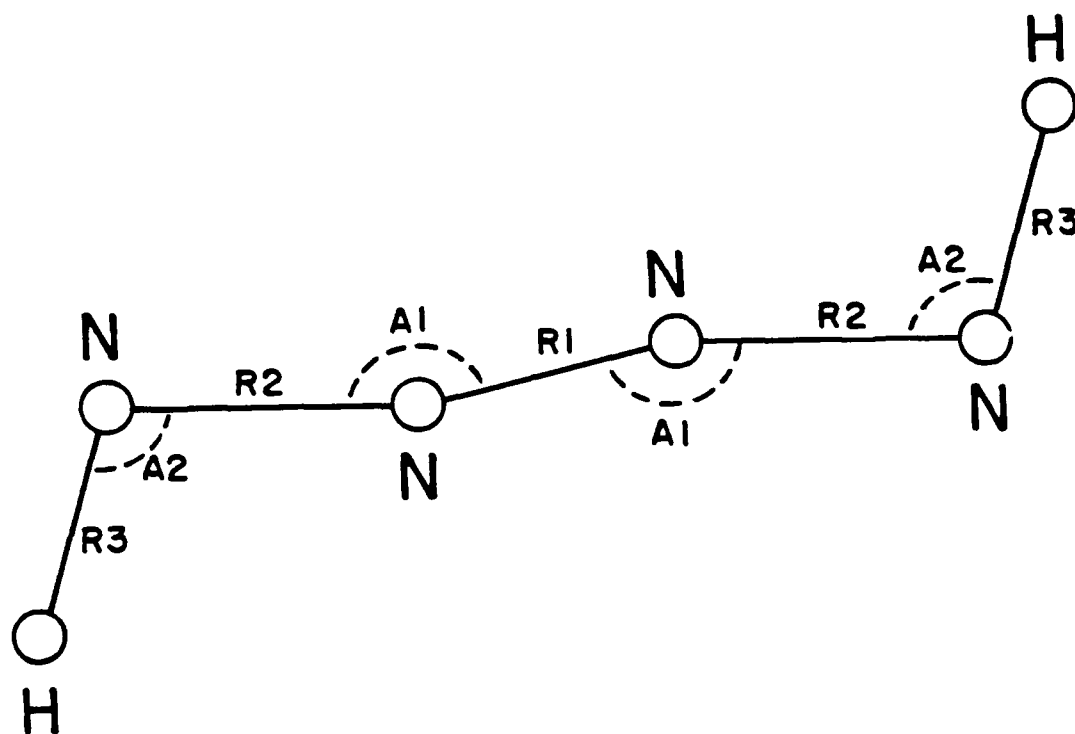
$R1 = 1.091182$
$R2 = 1.286423$
$R3 = 1.006396$
$A1 = 167.684971°$
$A2 = 106.236127°$
Total Energy $= -218.7010918$

HEAT OF FORMATION $= .3136350$ Hartrees $= 8.5309$ eV

SPECIFIC ENTHALPY $= 14.17$ MJ/kg

Figure A23. SCF 6-31G* geometry and energy of trans N_4H_2.

Trans N_4F_2
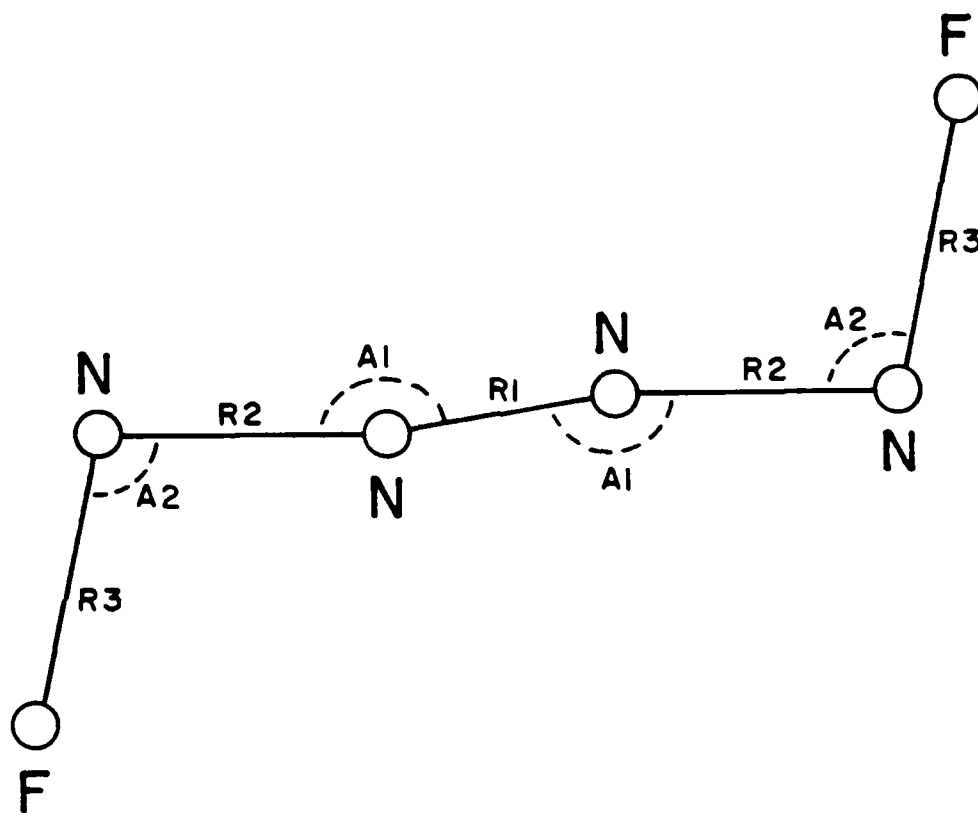
R1 = 1.083667
R2 = 1.343208
R3 = 1.383503
A1 = 170.891152°
A2 = 101.687974°
Total Energy = -416.2192904

HEAT OF FORMATION = .3463653 Hartrees = 9.4211 eV

SPECIFIC ENTHALPY = 9.66 MJ/kg

Figure A24. SCF 6-31G* geometry and energy of trans N_4F_2.

Trans N_4B_2
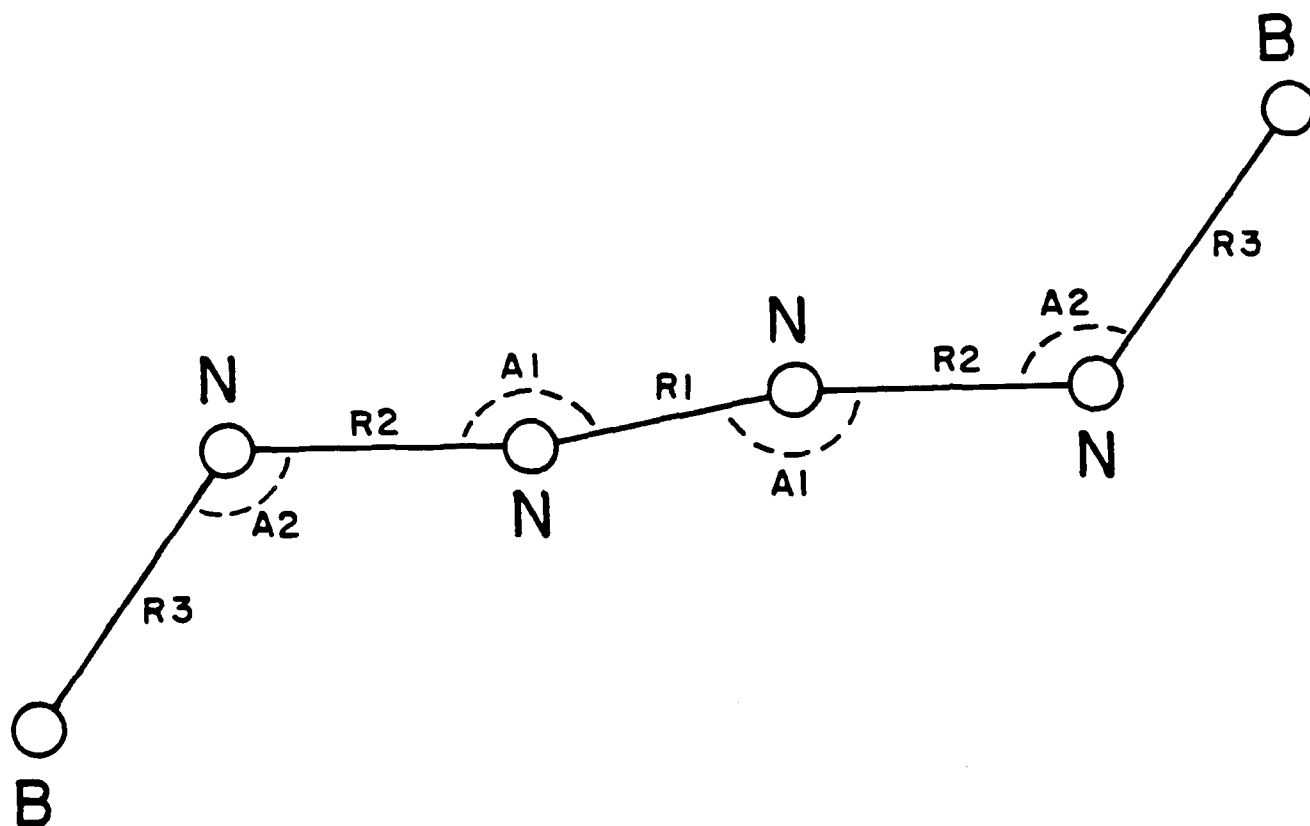
R1 = 1.091865
R2 = 1.247395
R3 = 1.399269
A1 = 169.835427°
A2 = 125.449998°
Total Energy = -266.8064233

HEAT OF FORMATION = .2389873 Hartrees = 6.5005 eV

SPECIFIC ENTHALPY = 8.07 MJ/kg

Figure A25. SCF 6-31G* geometry and energy of trans N_4B_2.

Trans $N_2H_2O_2$
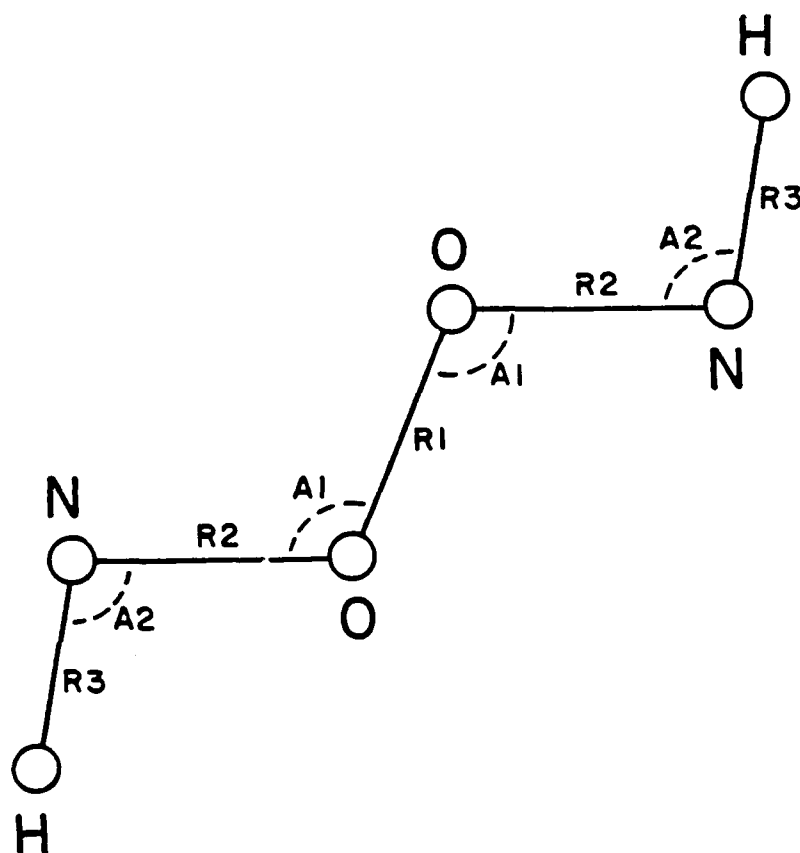
R1 = 1.260825
R2 = 1.300229
R3 = 1.005899
A1 = 112.956557°
A2 = 99.796521°
Total Energy = -259.3462083

HEAT OF FORMATION = .3228287 Hartrees = 8.7809 eV

SPECIFIC ENTHALPY = 13.65 MJ/kg

Figure A26. SCF 6-31G* geometry and energy of trans $N_2H_2O_2$.

Trans $N_2F_2O_2$
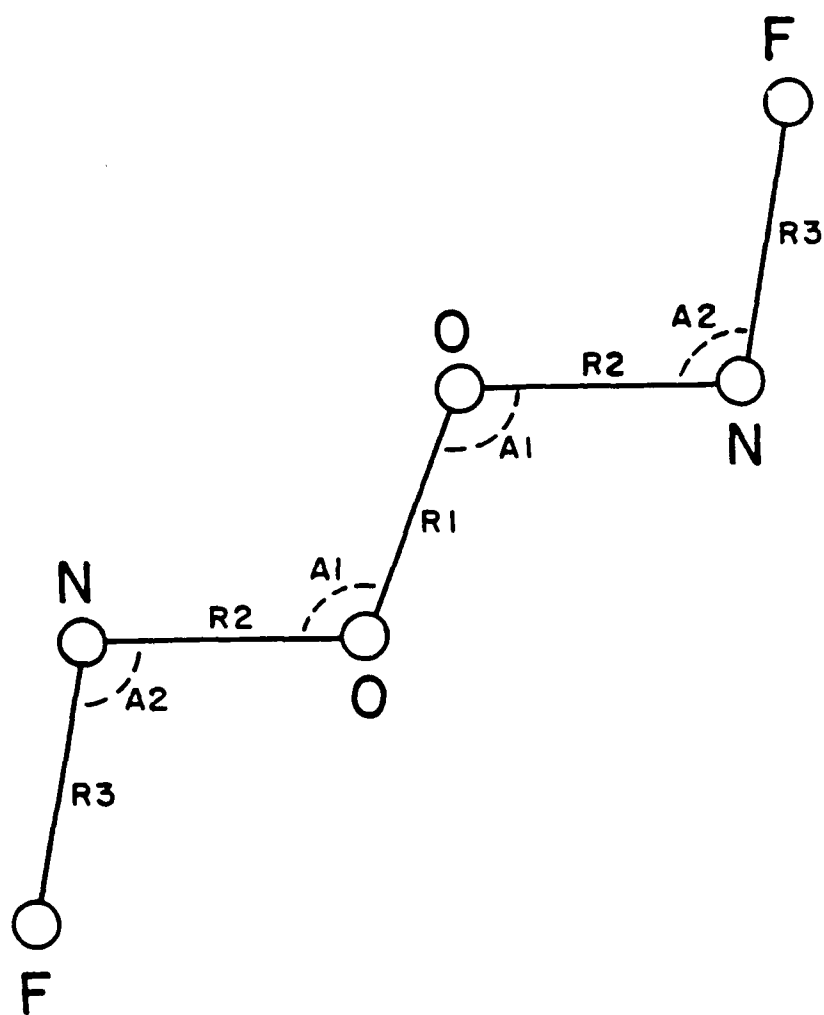
$R1 = 1.263938$
$R2 = 1.311162$
$R3 = 1.338081$
$A1 = 111.576175°$
$A2 = 100.261987°$
Total Energy $= -456.9093693$

HEAT OF FORMATION = .3105966 Hartrees = 8.4482 eV

SPECIFIC ENTHALPY = 8.31 MJ/kg

Figure A27. SCF 6-31G* geometry and energy of trans $N_2F_2O_2$.
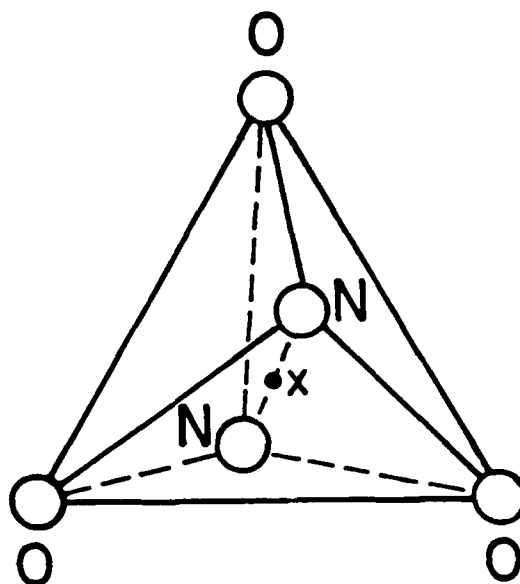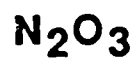
N_2O_3

$$d_{OO} = 1.94122$$
$$d_{NO} = 1.41942$$
$$\text{Total Energy} = -333.0304189$$

HEAT OF FORMATION = .3109202 Hartrees = **8.4570 eV**

SPECIFIC ENTHALPY = 10.72 MJ/kg

Figure A28. SCF 6-31G* geometry and energy of N_2O_3.
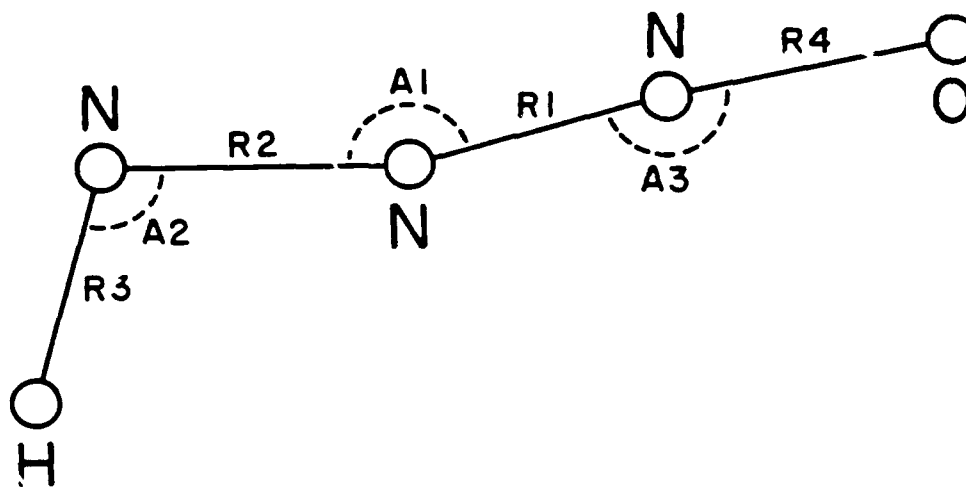
HN₃O

$$R1 = 1.092224$$
$$R2 = 1.27851$$
$$R3 = 1.00633$$
$$R4 = 1.20902$$
$$A1 = 165.835654°$$
$$A2 = 105.853619°$$
$$A3 = 176.956754°$$
$$\text{Total Energy} = -238.5498836$$

HEAT OF FORMATION = .2285844 Hartrees = 6.2175 eV

SPECIFIC ENTHALPY = 10.15 MJ/kg

Figure A29. SCF 6-31G* geometry and energy of HN₃O.
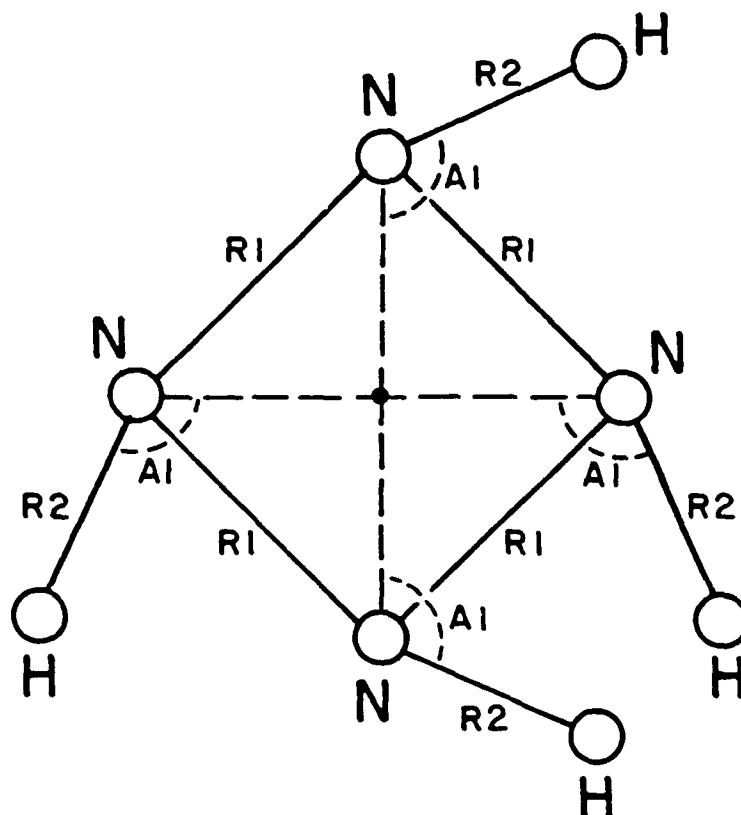
N_4H_4

R1 = 1.43963
R2 = 1.00326
A1 = 114.38979°
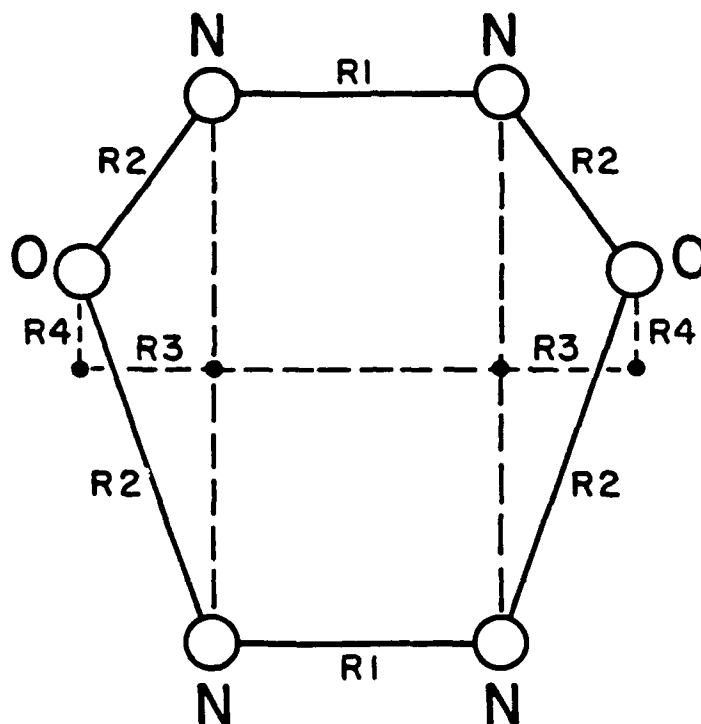Total Energy = -219.9495478

HEAT OF FORMATION = .1920068 Hartrees = 5.2226 eV

SPECIFIC ENTHALPY = 8.39 MJ/kg

Figure A30. SCF 6-31G* geometry and energy of N_4H_4.

N_4O_2 Boat

R1 = 1.19651
R2 = 1.37525
R3 = 0.57503
R4 = 0.49459
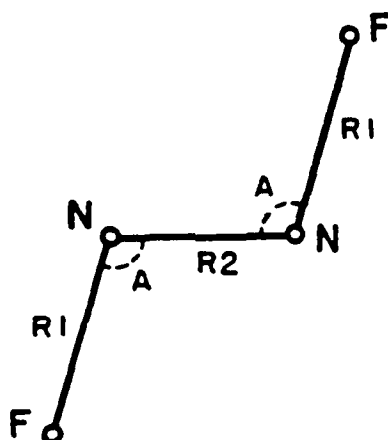Total Energy = -367.2158732

HEAT OF FORMATION = .2702855 Hartrees = 7.3518 eV

SPECIFIC ENTHALPY = 8.05 MJ/kg

Figure A31. SCF 6-31G* geometry and energy of the N_4O_2 boat.

Trans N_2F_2
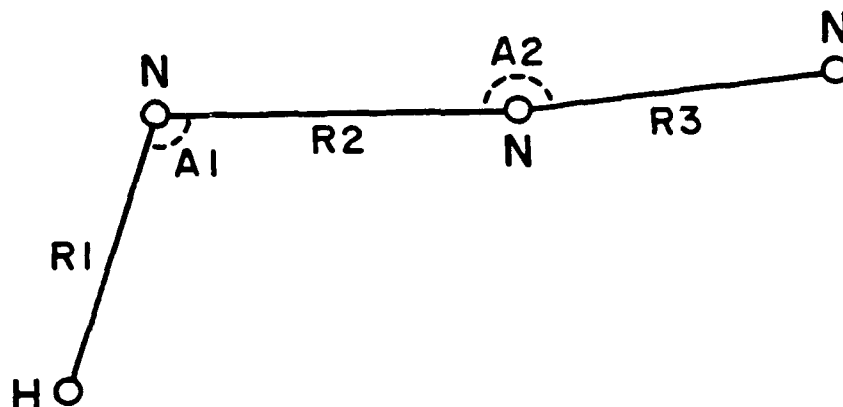

$$R1 = 1.338713$$
$$R2 = 1.193548$$
$$A = 106.744534°$$
$$\text{Total Energy} = -307.5820929$$

HEAT OF FORMATION = .0396133 Hartrees = **1.0775 eV**

SPECIFIC ENTHALPY = 1.57 MJ/kg

Figure A32. SCF 6-31G* geometry and energy of trans N_2F_2.

Hydrogen Azide (HN$_3$)

R1 = 1.005887
R2 = 1.238722
R3 = 1.09885
A1 = 108.242054°
A2 = 173.740826°
Total Energy = -163.8386958

HEAT OF FORMATION = .1406424 Hartrees = 3.8255 eV

SPECIFIC ENTHALPY = 8.57 MJ/kg

Figure A33. SCF 6-31G* geometry and energy of hydrogen azide (HN$_3$).

Fluorine Azide (FN₃)
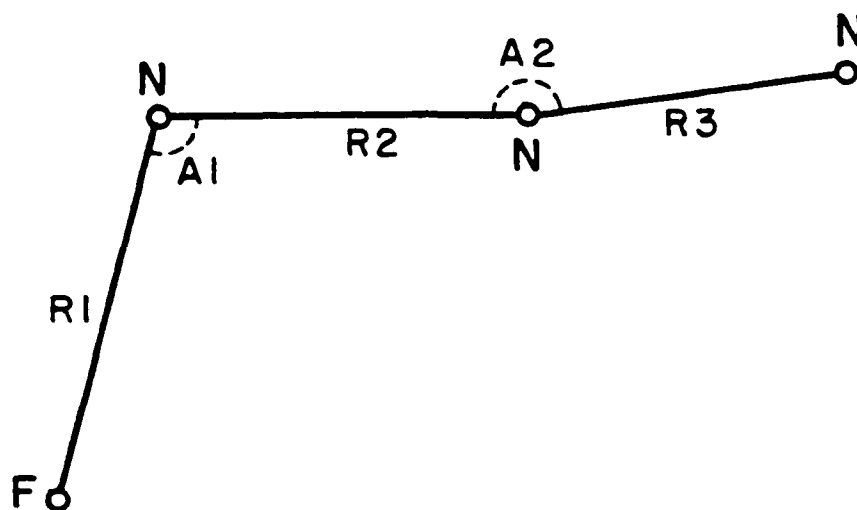
R1 = 1.3819
R2 = 1.2536
R3 = 1.0995
A1 = 104.33°
A2 = 173.99°
Total Energy = -262.6024876

HEAT OF FORMATION = .1523150 Hartrees = 4.1430 eV

SPECIFIC ENTHALPY = 6.54MJ/kg

Figure A34. SCF 6-31G* geometry and energy of fluorine azide (HN₃).